AD NUMBER

AD483277

LIMITATION CHANGES

TO:

Approved for public release; distribution is unlimited.

FROM:

**Distribution authorized to U.S. Gov't. agencies and their contractors;
Administrative/Operational Use; JAN 1966. Other requests shall be referred to Air Force Cambridge Research Laboratories, USAF Bedford, MA.**

AUTHORITY

AFCRL per ltr, 22 Dec 1971

MC 63-78-R2

AN INJECTION SYSTEM FOR ALLEVIATION OF RADIO BLACKOUT DURING RE-ENTRY

R. EARL GOODD
JOSEPH J. ROSSI

CONTRACT NO. AF19(628)-3852
PROJECT NO. 4642 TASK NO. 464202

FINAL REPORT
14 OCTOBER 1964 TO 14 DECEMBER 1965

JANUARY 1966

PREPARED
FOR
AIR FORCE CAMBRIDGE RESEARCH LABORATORIES
OFFICE OF AEROSPACE RESEARCH
UNITED STATES AIR FORCE
BEDFORD, MASSACHUSETTS

MITHRAS, INC.
AEROTHERMODYNAMICS - ELECTROMAGNETICS - QUANTUM PHYSICS
701 CONCORD AVENUE, CAMBRIDGE, MASS. 02138

MITHRAS, INC.
701 Concord Avenue
Cambridge, Massachusetts
02138

AFCRL-66-160

MC 63-78-R2

AN INJECTION SYSTEM FOR ALLEVIATION OF RADIO BLACKOUT DURING RE-ENTRY

by

R. Earl Good
Joseph J. Rossi

Contract No. AF19(628)-3852

Project No. 4642

Task No. 464202

Scientific Report No. 2

14 October 1964 to 14 December 1965

January 1966

Prepared
for

Air Force Cambridge Research Laboratories
Office of Aerospace Research
United States Air Force
Bedford, Massachusetts

FOREWORD

This report was prepared by MITHRAS, Inc., Cambridge, Massachusetts, for the Microwave Physics Laboratory, Air Force Cambridge Research Laboratories, Office of Aerospace Research, USAF, Bedford, Massachusetts, under Contract AF 19(628)-3852. The work was initiated by Mr. Walter Rotman and monitored by him and Mr. John F. Lennon.

The investigation leading to the results reported in this report were conducted during the period 14 October 1964 to 14 December 1965, and were directed by Mr. Jacques A. F. Hill and carried out by Mr. Joseph J. Rossi and Mr. R. Earl Good. This report was written by Mr. Joseph J. Rossi and Mr. R. Earl Good.

ABSTRACT

This report outlines method of creating a window for radio communication through a re-entry plasma sheath. The results of non-equilibrium numerical calculations illustrate that the injection of a coolant gas will reduce the plasma sheath temperature but will not reduce the free electron density or plasma frequency. Plasma electron density can be reduced, however, by attachment to electrophilic gases. The chemical rates of attachment are computed; and criteria are developed which specify the amount of electrophilic gas required to reduce the electron density a specified amount in a given time. As a practical application, a gas injection system for the total alleviation of S-band blackout throughout the re-entry of a Trailblazer II vehicle would have a total charged weight of 3.4 lbs., a volume of 215 $in.^3$, and would discharge 0.28 lbs. of SF_6 during re-entry. With a pulsed injection system, an even smaller system can be used.

TABLE OF CONTENTS

TABLE OF CONTENTS (Continued)

LIST OF TABLES

LIST OF ILLUSTRATIONS

LIST OF ILLUSTRATIONS (Continued)

LIST OF SYMBOLS

A	frequency factor
A_2	cross section area in flow field
A_i	atom or molecule of species i
C_Ω	mixing factor
C_P	specific heat
d	jet exit diameter
E	activation energy
E_a	electron affinity
E_o	zero-point energy
(e^-)	electron number concentration
(F)	fluorine number concentration
g_n	electron degeneracy
h	Planck constant
H	enthalpy
k	rate constant
k	Boltzmann constant
K	equilibrium constant
m	molecular weight
m	mass
$\dot{m}_o$	mass flow of jet
M	Mach Number
n	number of moles per gram
N_o	Avogadro's number
P'	partial pressure
P	pressure

LIST OF SYMBOLS(Continued)

$Q(A_i)$	partition function
s	streamline distance
t	time
T	temperature
U	velocity
x	position
(X)	third body
y	flow field thickness
ϵ_n	electron excitation level
χ	mole fraction
Δ	jet penetration distance
ρ	density
σ	jet injection angle
λ	inverse of the distance required to achieve equilibrium

Subscripts

0	initial conditions
1	undisturbed air
2	two body dissociative attachment reaction or normal shock values
3	three body direct attachment or conditions ahead of jet

LIST OF SYMBOLS (Continued)

D	molecular dissociative reaction
e	electron
j	jet
∞	free stream
c	coolant
a	air
t	total conditions
ex	exit conditions
f	final conditions
s	shoulder conditions

1. INTRODUCTION

Plasma blackout of radio communications during re-entry is a problem so formidable that it has become an accepted phenomenon during the Mercury and Gemini programs. Blackout has, so far, been tolerated on the assumption that the few minutes of lost communications are not crucial. In future missions such as Apollo, however, communications losses during re-entry will be quite critical since the blackout will persist for tens of minutes and could therefore threaten the safety and control of the vehicle during this maneuver.

Essentially, radio blackout is caused by the presence of large concentrations of free electrons in the flow field. Figure 1 illustrates the attenuation that occurs around a blunt body from the flow of ionized air; the air that is ionized at the front of the vehicle expands around the body and cools. If the air could at all times be in thermodynamic equilibrium, the attenuation would be reduced as illustrated by the bottom trace. Unfortunately, however, the numerous molecular, atomic, and electronic species found in air react together at a finite rate which, in hypersonic flight, is too slow to keep up with the rate of density expansion around the body. Equilibrium cannot thus be maintained, and attenuation occurs at a level somewhere between the two top traces of frozen and non-equilibrium flow. The extreme level of attenuation shown by the top line occurs when no specie change occurs and the flow is considered frozen.

Creating a transmission window through the plasma sheath around a re-entry vehicle requires a technique for reducing the electron density in the regions of the air flow surrounding the antenna. The obvious way to reduce the electron density is to cool the air flow, either by aerodynamic shaping or by coolant injection. Unfortunately, the flow can be cooled without an accompanying reduction in the plasma electron density since the inherent electron recombination rate is too slow for thermodynamic equilibrium to be achieved anywhere near the point of coolant injection. To speed up the

recombination rate an additive must be found to serve as a new "sink" for electrons; one possibility is the removal of electrons by electrophilic gas attachment.

The best known electrophilic gases, the halogens – chlorine, fluorine, iodine and bromine – have a large affinity for electrons. In fact, equilibrium calculations show the halogens to be capable of reducing the plasma electron concentrations several orders of magnitude when the plasma has cooled below 3000°K. Furthermore, halogen gases are commercially available in many molecular compounds such as SF_6, CCl_4, Freon-14, Freon-12 and Cl_2, and these compounds are themselves electrophilic and can easily be injected into the plasma, some under their own vapor pressure.

Upon injection into the plasma, electrophilic gases attach electrons by one of two processes: (1) direct three body attachment between the halogen atom and electron, or (2) dissociative attachment between the halogen molecule and electron. Which reaction is dominant depends on the flight altitude and location of the injection point in the flow. For injection into highly expanded flow, the frozen electron density will be reduced by dissociative attachment, and injection at the stagnation point will favor three body direct attachment.

2. INJECTION SYSTEM CONCEPT

To cool a supersonic flow by means of jet injection of electrophilic gas, the maximum lateral penetration must be achieved with as little disturbance to the main flow as possible. The specific method adopted is to expand the injected fluid to a high Mach No. and to a pressure which balances the pressure of the external stream. This correctly expanded jet is directed across the main stream so that the momentum carries the jet fluid well out from the orifice before the fluid is swept downstream. The fluid spreads into the stream by turbulent mixing, and then gradually mixes with the external stream to fill the shock layer adjacent to the radio antenna as shown in Figure 2.

Multiple jets are used so that the airstream is not blocked; if the airstream were blocked a strong standing shock wave would be set up in front of the field of jets. A plan view of the jets is shown in Figure 3. Each tiny gas jet creates a shockwave in front of it which heats up only a small portion of the oncoming airflow, most of which passes around the jet unchanged, and is gradually mixed into the jet flow containing the electrophilic additives. In this way, the jets do not alter the basic airflow while adding the electrophilic gases.

2.1 Jet Size

The MITHRAS technique (Ref. 1) for designing the individual jet size and Mach No. to achieve the desired penetration is presented below. The behavior of the flow, the mixing and the penetration distances will depend on injection Mach No., angle, fluid density, and free stream properties.

In Figure 4, a circular jet is represented by an expanding, curving tube in the external stream. The tube will contain more and more external stream air entrained by turbulent mixing as it moves outward. Near the orifice, the upstream or leading edge will act like a bluff obstacle in the main flow,

and there will be a normal shock in the flow before it spreads around the jet tube and closes behind it. Actually, part of the jet fluid will be torn away from the tube and carried downstream, thus distorting the circular form and reducing the total mass of the jet. The impact of the free stream on the jet tube will cause it to start curving downstream. As the jet progresses, it picks up mass by entraining external stream air while maintaining a constant momentum. Since the jet will be curving, a centrifugal force will appear in the force equations. As the jet tube turns, it presents a different angle to the external stream, thus changing the impact which the external stream exerts on it.

The jet penetration is determined from a solution of the force equations, and the growth rate of the mass flow in the jet is given by Ricou and Spalding (Ref. 2). Solutions of the force equations are given by Adams and Rossi (Ref. 1).

$$y/d = \bar{\alpha} \int \sin \sigma \, (\bar{s}, \bar{c}) \, d\bar{s} \tag{2.1}$$

$$x/d = \bar{\alpha} \int \cos \sigma \, (\bar{s}, \bar{c}) \, d\bar{s} \tag{2.2}$$

where

$$\bar{\alpha} = 2.99 \sqrt{\gamma_j} \, \frac{M_{j_o} \sin \sigma_o}{\left(\rho_2/\rho_1\right)^{1/2}} \tag{2.3}$$

$$\bar{c} = 2.47 \left(\frac{\rho_1}{\rho_2}\right) \tag{2.4}$$

$$\bar{s} = (s/d) \left(\frac{1}{\bar{\alpha}}\right) \tag{2.5}$$

Solutions for jet penetration (Figures 5, 6 and 7) were obtained for the injection of SF_6 but, unfortunately, there are no previous experiments with which to compare the present findings and theory. Several reports are available on penetration from underexpanded sonic jets, and References 3 and

4 present height to diameter ratios of between 10 and 50 for incorrect expanded flow. As already mentioned, though, the injection of electrophilic gases requires correctly expanded flows so that the jet will be as small as possible to not form a strong shock. Therefore, wind tunnel experiments must be conducted to observe the penetration of correctly expanded jets.

Jets can be designed for a specific application by developing design charts from the numerical results presented in Figures 5, 6 and 7. The jet mass flow rate of SF_6 through a sonic or supersonic nozzle can be specified as

$$\dot{m}_{SF_6} = \frac{1.09\, P_t\, A^*}{\sqrt{T_t}} \tag{2.6}$$

where A^* is the jet throat area and $\dot{m}_{SF_6}$ is the jet mass flow rate of SF_6. The jet exit diameter, d_{ex}, can be obtained by specifying the ratio, $\dot{m}_{SF_6}/P_{ex}$.

$$\frac{\dot{m}_{SF_6}}{P_{ex}} = \frac{1.09\pi}{4} \frac{d_{ex}^2}{\sqrt{T_o}} \left(\frac{A^*}{A_{ex}}\right) \frac{P_t}{P_{ex}} \tag{2.7}$$

where A_{ex} and P_{ex} are the jet exit area and pressure. The ratios

$$\left(\frac{A^*}{A_{ex}}\right) \quad \text{and} \quad \left(\frac{P_t}{P_{ex}}\right)$$

are obtained from isentropic flow tables as a function of jet Mach No. and the ratio of specific heats of the injected gas.

For a correctly expanded jet, the jet exit pressure is matched to

the air pressure immediately ahead of the jet, and the jet exit diameter is then given as

$$d_{ex} = 5.22 \sqrt{\frac{\dot{m}_{SF_6}}{P_3}\left(\frac{A_{ex}}{A^*}\right)\left(\frac{P_{ex}}{P_t}\right)} \qquad (2.8)$$

where $T_o = 540^\circ R$.

The jet exit diameter and jet Mach No. uniquely determine the maximum penetration distance. Thus the relationship obtained from Figure 5 and additional calculations is shown in Figure 6 as

$$\Delta = d_{ex}\, f(M_j,\ M_\infty, \gamma_j, \sigma_o = 90^\circ) \qquad (2.9)$$

The change in penetration distance brought about by a reduction in the injection angle, σ_o, is shown in Figure 7. Thus, a design chart can be formed (Figure 8) using Equation 2.8 and Figures 6 and 7 in the form of

$$\frac{\dot{m}_{SF_6}}{P_3} = \Delta^2\, f(M_j,\ M_\infty,\ \gamma_j,\ \sigma_o = 90^\circ) \qquad (2.10)$$

2.2 Mass Flow Requirements

Mass flow must satisfy the following three requirements:

1. The number density of SF_6 must exceed the electron number density ($\chi_{SF_6} >> \chi_{el}$).
2. There must be enough SF_6 to obtain a fast attachment rate.
3. Enough mass must be injected to obtain the desired penetration of the flow field.

2.3 System Weight

The electrophilic gas is stored as a liquid and, in most applications, the vapor pressure is more than adequate to form the supersonic gas jet. Consequently, the injection system consists of a pressure vessel for gas storage, nozzle, on/off valve, and metering valves. Since small pressure vessels are constructed with typical weight-to-volume ratios of 0.05 lbs/in^3, a storage vessel to hold 0.5 lb. of liquid SF_6 (specific gravity = 1.6) would weigh 1.5 lbs. The valves would add another 1.5 lbs. thus giving a total system weight of 3.0 lbs. for 0.5 lb. of SF_6 or a system-to-gas weight ratio of 6.0. Specific system weights will be given in Section 5 for a Trailblazer II vehicle.

3. NON-EQUILIBRIUM COOLING

In order to find a means of removing the plasma sheath electrons blocking communications during re-entry, the thermodynamic state of the ionized plasma layer must be known, and then a way must be found to cool this flow to a state in which few electrons are present. The flow of air over the body surface can be assumed to be in any of the three following states:

1. Perfect gas
2. Equilibrium gas
3. Non-equilibrium gas

Although the perfect gas assumption can contribute no electrons to the flow, it is nonetheless useful since it is the first step towards more complex assumptions.

An analysis of the one-dimensional mixing and cooling of a streamtube with the assumption of both a perfect and an equilibrium gas has been completed in a previous report (Ref. 1). The final state in the cooling process for the perfect gas case was achieved directly, although the final temperature had to be specified to achieve a solution for the equilibrium gas case. A method of analysis must now be determined for the more realistic condition of non-equilibrium cooling.

3.1 Two Streamtube Formulation

The non-equilibrium flow of a Nitrogen-Oxygen mixture down a streamtube can be calculated with the equations presented by Vincenti (Ref. 5) if the pressure along the streamtube is specified. The formulation for this non-equilibrium flow has been programmed on a 7090 computer, and thermodynamic properties as a function of streamtube distance can be derived by following the various chemical reactions in the streamtube. Cooling the flow with allowances for non-equilibrium conditions can be determined by including in the program a psuedo reaction describing the interchange of energy between an injected coolant and non-equilibrium flow. This is done schematically in the following way:

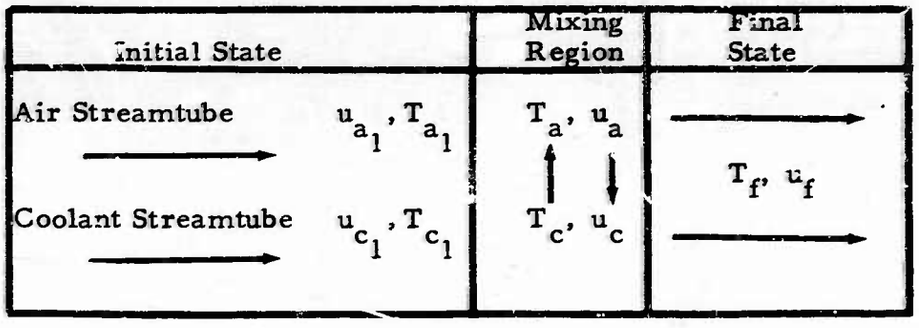

The non-equilibrium Nitrogen-Oxygen reactants are contained in the air streamtube flowing adjacent to the coolant streamtube. The coolant and the airstream exchange energy in the mixing region until they both reach the same final energy state; however, the coolant is assumed to remain a non-reacting gas. Conservation of energy and momentum between the two adjacent streamtubes is stated below:

$$dH_a + C_Q dH_c = 0 \qquad (3.1)$$

$$du_a + C_Q du_c = 0 \qquad (3.2)$$

with C_{Q_1} being defined as the ratio of injected coolant to initially undisturbed air

$$C_{Q_1} = \frac{\dot{m}_c}{\rho_1 u_1 A_1} \tag{3.3}$$

Both the air and coolant are assumed to undergo a relaxation process in the mixing region as follows:

$$u_a = u_f + (u_{a_1} - u_f)\, e^{-\lambda x} \tag{3.4}$$

$$u_c = u_f(1.0 - e^{-\lambda x}) \tag{3.5}$$

where

λ = scaling factor
u_c = final cooled state
x = streamtube distance

The final velocity, u_f, is unknown; however, by forming the derivatives

$$du_a/dx, \quad du_c/dx$$

and substituting these values in Equation 3.2, u_f can be determined to be:

$$u_f = \left(\frac{u_{a_1}}{1 + C_{Q_1}} \right) \tag{3.6}$$

This is the same value for the final velocity as that found for both the perfect and equilibrium gas cases. That this is so is a check on the validity of Reference 1 since, regardless of what non-isentropic process is occurring between two stations, the momentum equation holds considering flow properties at stations far from this region.

The relaxation process for the temperature of the airstream and the coolant can be postulated as follows:

$$T_a = T_f + (T_{a_1} - T_f)\, e^{-2\lambda x} \tag{3.7}$$

$$T_c = T_f - (T_f - T_{c_1})\, e^{-2\lambda x} \tag{3.8}$$

$$u_a = u_f + (u_{a_1} - u_f)\, e^{-\lambda x} \tag{3.4}$$

$$u_c = u_f(1 - e^{-\lambda x}) \tag{3.5}$$

where λ is a scaling factor which determines the rate of cooling. Derivatives of du_a/dx, du_c/dx and dh_a/dx are now formed as a function of the temperature and velocity difference.

Unlike the air and coolant streamtube velocities the temperature has been assumed to decay as $e^{-2\lambda x}$ since this assumption yielded the simplest closed form solution for both the final temperature and velocity. The derivative for the static enthalpy of the airstream can be formed using the definition for the static enthalpy of a calorically perfect gas,

$$h_a = C_{P_a} T_a \tag{3.11}$$

and eliminating T_f from the derivative (see Appendix A). The result is

$$\frac{dh_a}{dx} = -\frac{2C_{Q_1}\lambda}{1 + C_{Q_1}\left(\frac{C_{P_c}}{C_{P_a}}\right)}\left\{ C_{P_c} - \frac{u_1^2}{2(1 + C_{Q_1})(T_{a_1} - T_{c_1})} \right\} (T_a - T_c) \tag{3.12}$$

In the same manner, derivatives for du_a/dx, and du_c/dx can be formed from Equations 3.4 and 3.5 and the sum of these two equations. These derivatives are:

$$\frac{du_a}{dx} = - \frac{\lambda C_{Q_1}}{1+C_{Q_1}} (u_a-u_c) \quad (3.13)$$

$$\frac{du_c}{dx} = + \frac{\lambda}{1 + C_{Q_1}} (u_a-u_c) \quad (3.14)$$

Having formed derivatives of static enthalpy for air, and derivatives of velocity for both air and coolant as a function of the difference in coolant and airstream temperatures and velocities, a numerical iteration procedure can be established to determine new values of air and coolant velocities and airstream static enthalpy. The static enthalpies, with pressure assumed constant for both streamtubes, will yield new values of the coolant and air temperatures which, in turn, will allow calculation of a new value of dh_a/dx. As the difference (T_a-T_c) and (u_a-u_c) approach zero, the iteration will stop and these values will be the final ones.

3.2 Freezing Criterion

A cooling rate matching or exceeding the chemical reaction rates of the air species comprising the air streamtube must be determined to get an equilibrium cooling solution. Since electrons are the most important chemical specie from a communication standpoint, a freezing criterion will be chosen which will keep electrons in equilibrium while cooling is occurring. To do this, an equilibrium electron concentration and its rate of change as a function of distance must be found and compared to the rate of change of

electrons given by the following formula taken from Appendix B:

$$\frac{de^-}{dx} = \frac{\rho}{N_o \cdot u} \left[k_f(N)(O) - k_b(e^-)^2 \right] \tag{3.15}$$

where:

(e^-) = specie in particles/cc

k_f = forward reaction constant (cm^3/mole sec) for

$N + O \rightarrow NO^+ + e^-$

k_b = backward reaction constant (cm^3/mole sec) for

$N + O \leftarrow NO^+ + e^-$

u = air streamtube velocity.

Since the primary interest is in cooling cases for which

$$\frac{de^-}{dx} < 0$$

the ed equilibrium rate of change of electrons will be compared with

$$\left(\frac{de^-}{dx}\right)_{eq} = \frac{k_b(e^-)^2}{N_o \cdot u} \tag{3.16}$$

The assumed equilibrium electron concentration is found in the following way. The final cooled equilibrium state is known from previous research, (Ref.1) and the equilibrium properties of the streamtube are expected to vary in a way similar to the previously obtained perfect gas cooling solutions. Therefore, an equilibrium cooling case, in which the final state is known by using the methods presented in Reference 1, can be compared with a perfect gas cooling calculation at the same initial enthalpy (shown in Figure 9). Thus the assumed variation of the thermodynamic variables for the equilibrium case can be determined. The enthalpy, temperature, pressure

and velocity thus found (Figure 10) allows calculating electrons as a function of non-dimensionalized distance λx (Figure 11) from plasma charts. The equilibrium electron concentration thus found is then differentiated to determine

$$\frac{de^-}{d(\lambda x)} = \frac{1}{\lambda} \left(\frac{de^-}{dx}\right)_{eq} \tag{3.17}$$

where λ^{-1} represents, in effect, the distance required to achieve equilibrium recombination. The right hand side of Equation 3.16 can now be calculated since the equilibrium electron variation is known and since, k_b, the backward rate constant in the reaction describing the production of electrons, is simply a function of temperature. By comparing the postulated equilibrium variation of electrons

$$\frac{1}{\lambda} \left(\frac{de^-}{dx}\right)_{eq} \tag{3.18}$$

with the actual rate of change of electrons as defined by

$$\frac{de^-}{dx} = \frac{k_b (e^-)^2}{N_o \cdot u} \tag{3.19}$$

λ can be selected such that

$$\frac{1}{\lambda} \left(\frac{de^-}{dx}\right)_{eq} \leq \frac{k_b (e^-)^2}{N_o \cdot u} \tag{3.20}$$

and thus have equilibrium flow cooling, or λ can be selected such that

$$\frac{1}{\lambda} \left(\frac{de^-}{dx}\right)_{eq} > \frac{k_b (e^-)^2}{N_o \cdot u} \tag{3.21}$$

and thus have frozen cooling. This comparison is shown in Figure 12.

3.3 Numerical Results

As a check on the 7090 computer program, runs were made attempting to duplicate the computations made on a Recomp III computer for a known perfect gas case. This was done by setting the rate constants for the non-equilibrium reactions equal to zero so that the equations describing the non-equilibrium flow reduce to a perfect gas case and a valid comparison could be made. The results of these runs are plotted in Figure 13 with the perfect gas results from Reference 1. The initial difference in the temperature and velocity curves is due to a difference in the choice of computation step size for the 7090 and Recomp III programs.

Similarly a check was made for an equilibrium gas cooling case run at the condition shown in Figure 14. By using the results of an assumed equilibrium variation of electrons, derived by knowing the thermodynamic states during mixing for the similar (constant initial enthalpy) perfect gas case, a cooling rate, λ, was picked such that the flow remained in equilibrium throughout. With this $\lambda = .01\ cm^{-1}$, Figure 13 shows that the final cooled state should be reached at approximately $\lambda x = 3.0$; for this present case this would mean 300 cm downstream of initial coolant injection. Since the present computer program involves a Runge-Kutta integration procedure which requires that the computation step size be $\leq 1.10^{-2}$ cm to control the propagation of errors, only the first $1000^{\circ}K$ drop in temperature was computed. The results are shown in Figure 14 and compared to a known equilibrium solution.

An analysis of the freezing criterion for conditions

$T_1 = 5075^{\circ}K$

$P_1 = 0.1$ atm

$C_Q = .966046$

is shown in Figure 15. This analysis indicates that, unless the cooling

length λ^{-1} is greater than 1000 cm, non-equilibrium cooling would occur. To verify this observation, computations were made at $\lambda^{-1} = 10$ with the results shown in Figures 16 and 17. Although the temperature dropped considerably from its initial value (Figure 16) the various specie concentration (Figure 17) remain essentially unchanged. In fact, although the electron concentration dropped by a factor of approximately 10^2 for the non-equilibrium case, the drop would have been much greater (i.e., 10^5) had equilibrium occurred. Therefore, even though the temperature is cooled within 10 cm, the electron concentration drops only by a factor of about 10^2 instead of the 10^5 reduction possible if equilibrium had been reached. A cooling length of 1000 cm would be required to achieve equilibrium. This is an unreasonable distance and thus shows that cooling techniques are not an effective weapon in combatting radio blackout.

4. ELECTRON ATTACHMENT TO ELECTROPHILIC GASES

Essentially electrophilic gases are those which form stable negative ions in the presence of electrons. The phenomenon of electron attachment to electrophilic atoms and molecules has been stud[illegible] decades and must involve energy emission since the negative ion is at [illegible]wer energy level than the original neutral species. The energy emitted to attach an electron is known as the electron affinity, E_a, and those atoms and molecules having an electron affinity are tabulated in Table I; chlorine and fluorine atoms have the highest affinity of any known material.

Electron attachment can occur either by three body attachment reaction such as

$$F + X + e^- \rightleftarrows F^- + X \tag{4.1}$$

or by dissociative attachment reaction such as

$$SF_6 + e^- \rightleftarrows SF_5^- + F \tag{4.2}$$

The negative ion is then neutralized in collision with the positive ions. The number of free electrons that can be removed from a plasma can be determined from equilibrium calculations. The equilibrium constant is defined as the ratio of the concentration of products over the concentration of reactants. For three body attachment, the equilibrium constant is

$$K_{3C} = \frac{(F^-)}{(F)\,(e^-)} \tag{4.3}$$

and for two body dissociative attachment, the constant is

$$K_{2C} = \frac{(SF_5^-)\,(F)}{(SF_6)\,(e^-)} \tag{4.4}$$

where the brackets represent molecules/cc. The equilibrium constant is related to the partition functions by

$$\ell n\, K_c = - \frac{\Delta E_o}{kT} + \sum_{i=1}^{n} \Delta\gamma_i\, \ell n\, Q(A_i) \qquad (4.5)$$

where $\Delta\gamma_i$ is the difference in the stoichiometric coefficients of the products and the reactants. The ΔE_o is the difference in the zero point energy between the products and the reactants. The partition function is defined as the product of the partition functions for translation, rotation, vibration, and electronic energy states, and is given below for translation (Q_t) and electronic states (Q_e), respectively:

$$Q_t = \left(\frac{2\pi\, m\, kT}{h^2} \right)^{3/2} \qquad (4.6)$$

$$Q_e = \sum_{n=1}^{\infty} g_n\, e^{-\epsilon_n/kT} \qquad (4.7)$$

where k is Boltzmann's constant.

4.1 Equilibrium Attachment

The equilibrium number of attached electrons is independent of any attachment reaction and is a function only of temperature and pressure. Although the dissociative attachment reaction is a faster attachment path than molecular dissociation followed by atomic attachment, they both will eventually reach the same equilibrium condition.

The equilibrium constant for the three body fluorine attachment reaction can be written using Equations 4.5 through 4.7 and the constants in Table I, as follows:

$$K_{3c} = \frac{1}{2}\left(\frac{2\pi m_e kT}{h^2}\right)^{-3/2} \frac{e^{-E_a/kT}}{\Sigma g_n e^{-\epsilon_n/kT}} \qquad (4.8)$$

The difference in zero point energy between the negative ion and the atom is the electron affinity.

The electron concentration in the presence of halogen atoms was determined from the simultaneous solution of Equation 4.8 and the following equations for conservation of atoms and charge:

$$\begin{aligned} &(F) + (F^-) = (F)_o \quad \text{conservation of atoms} \\ &(F^-) + (e^-) = (e^-)_o \quad \text{conservation of charge} \end{aligned} \qquad (4.9)$$

Note that $(\ )_o$ denotes initial conditions.

The solution of these equations for the electron concentration is:

$$(e) = -\left(\frac{(F)_o - (e^-)_o + \frac{1}{K_{3c}}}{2}\right) + \sqrt{\left(\frac{(F)_o - (e^-)_o + \frac{1}{K_{3c}}}{2}\right)^2 + \frac{(e^-)_o}{K_{3c}}} \qquad (4.10)$$

The usual practice is to have the fluorine concentration much larger than the electron concentration since under this circumstance, fluorine is not appreciably consumed and the conservation of fluorine atoms can be neglected. Then the electron concentration is given as:

$$\frac{(e^-)}{(e^-)_o} = \frac{1}{K_{3c}(F)_o + 1} \qquad (4.11)$$

The order of magnitude of electrons removed by attachment to fluorine is shown in Figure 18. The striking feature of this figure is that almost no electrons are removed at temperatures above 3000°K. The results are presented in terms of the partial pressure of fluorine; the mole fraction of fluorine added is given by:

$$\chi = P'(F)/P_o$$

The inverse equilibrium constant for other electrophilic gases is shown in Figure 19. The halogen atoms are shown to be far superior to other atoms in their ability to attach electrons.

4.2 Relative Importance of Molecular and Electron Collisions in Dissociation of SF_6

The mode of electron attachment is determined by the relative speeds of molecular and electron collisions in dissociating SF_6 which occurs by the following reaction:

$$SF_6 + X \rightleftharpoons SF_5 + F + X \qquad (4.12)$$

The dissociation rate is specified for Equation 4.12 as

$$\frac{d(SF_6)}{dt} = - k_D (SF_6)(X) \qquad (4.13)$$

Integration of Equation 4.13, assuming constant air temperature and density, gives an exponential change in SF_6 concentration, e.g.:

$$(SF_6) = (SF_6)_o \; e^{-k_D(X)t_o} \qquad (4.14)$$

where (X) is the air concentration. The dissociation rate coefficient, k_D, is obtained from experiments. In the shock tube experiments (Ref. 6),

complete dissociation of SF_6 was observed to occur at some time prior to the ionization of air. If the rate determining step for the complete dissociation of SF_6 is the first step (Equation 4.12), then the rate coefficient can be specified from Equation 4.14, as follows:

$$k_D = \frac{1}{(X)t_o} \ln \frac{(SF_6)_o}{(SF_6)} \tag{4.15}$$

Substituting the observed ionization for the dissociation time, t_D, and assuming that the SF_6 is 99.9 percent dissociated, the dissociation coefficient at test conditions of 3840°K and 1.5 atm is given as

$$k_D = 4.3 \times 10^{-7} \qquad cm^3 \text{ molecules}^{-1} \text{ s}^{-1}$$

The temperature dependence of the rate coefficient can be determined by assuming a simple Arrhenius law, as follows:

$$k_D = A\, e^{-E/RT} \tag{4.16}$$

The activation energy for dissociation is the energy of the bond broken in the reaction. The first bond is the strongest, thus substantiating the assumption that the first step determines rate. With the bond energy for Equation 4.12 given in Table II as 85 kcal/mole, the rate coefficient can be specified as

$$k_D = 3.5 \times 10^{-10}\ e^{-85000/RT} \tag{4.17}$$

which is within a factor of two of the value obtained by direct observation of Cl_2 dissociation (Ref. 7). Oxidation reactions with SF_6 are possible and would speed up the dissociation (Ref. 8).

The rate coefficients for the dissociative attachment reaction, Equation 4.2, can be specified from electron beam experiments used to

measure attachment cross sections. The cross section for SF_6 is given in Reference 9 and is a function of the electron velocity. The rate coefficient is defined as

$$k_2 = \int_o^\infty U\ \sigma(U)\ dU\ . \qquad (4.18)$$

There is no exponential dependence since the activation energy for the dissociative attachment is essentially zero. This integral can be evaluated as a function of temperature assuming an appropriate velocity distribution. For illustration purposes, approximating the integral will be sufficient and, thus, the rate coefficient can be derived as follows:

$$k_2' = \overline{U}\ \sigma_{peak} \qquad (4.19)$$

where

$$\overline{U} = \sqrt{\frac{8kT}{\pi m_{el}}}$$

$$\sigma_{peak}\ (SF_6) = 2 \times 10^{-17}\ cm^2\ @\ E \simeq 0.1\ eV. \quad \text{(see note)}$$

E = electron energy at cross section peak.

Thus the dissociative attachment rate coefficient is given as

$$k_2' = 1.3 \times 10^{-11}\ \sqrt{T}\ cm^3\ molecules^{-1}\ s^{-1} \qquad (4.20)$$

Loss of electrons by resonance electron capture is insignificant at temperatures above 1000°K since the resonance capture cross section consists of a very narrow peak centered at about zero electron energy.

Note added in proof:

Cross sections as high as $2.6 \times 10^{-14}\ cm^2$ have been reported by Mahan and Young (Ref. 16). This would greatly increase the rate of dissociative attachment.

The relative importance of the two dissociative processes is obtained by plotting the ratio of the molecular dissociation rate to the dissociative attachment rate:

$$\delta = \frac{\left.\frac{d(SF_6)}{dt}\right|_{\text{molecular}}}{\left.\frac{d(SF_6)}{dt}\right|_{\text{electron}}} = \frac{-k_D(SF_6)(X)}{-k_2'(SF_6)(e^-)} \tag{4.21}$$

Substituting for Equations 4.13 and 4.19,

$$\delta = 35\, T^{-1/2}\ e^{-43000/T}\ \chi_e^{-1} \tag{4.22}$$

the mole fraction of electrons is defined

$$\chi_e = \frac{(e^-)}{(X)} \tag{4.23}$$

Equation (4.22) is plotted as a function of temperature in Figure 20 to illustrate that dissociative attachment is the dominant reaction for typical values of the electron mole fraction at temperatures below about 4000°K. Thus, in expanded flow regions where the temperature is low, the SF_6 will remove electrons by dissociative attachment. In the high temperature regions near the stagnation point, molecular dissociation is the predominant reaction and electrons can only be removed by three body attachment.

4.3 Dissociative Attachment Rate in Expanded Flow Regions

On many vehicles, the communications antennas are located aft of the vehicle nose in an expanded flow region. The air around the antenna will have expanded from a stagnation point condition and will be cool;

however the electron density will be large because the recombination rates are slow compared to the expansion rate. Thus, a large electron mole fraction exists in a cooled gas. An electrophilic gas injected into this type of flow will remove electrons by the dissociative process described earlier.

The rate of electron removal by dissociative attachment is given as

$$\frac{d(e^-)}{dt} = - k_2' (SF_6) (e^-) \qquad (4.24)$$

where ( ) represents molecules cm^{-3}. This expression is valid only until equilibrium is approached. At near equilibrium, reverse reactions will begin to be significant. The amount of electron density reduction is obtained by integrating Equation 4.24 assuming that the air temperature and density remain fixed. The concentration of SF_6 is also unchanged since the amount added greatly exceeds the electron density. Integrating Equation 4.24 also yields an exponential electron density decay of the form

$$(e^-) = (e^-)_o \exp \left[-k_2'(SF_6)(\Delta t) \right] \qquad (4.25)$$

By defining the concentration of SF_6 in terms of mole fraction of the air density and substituting the rate coefficient in Equation 4.20, the elapsed time to reduce the electron density by 100 by dissociative attachment, t_2^{100}, is given as

$$t_2^{100} \chi_{SF_6} = \frac{1.7 \times 10^{-11}}{\rho T^{1/2}} \qquad (4.26)$$

The attachment time, t_2^{100}, given in Equation 4.26, is plotted in Figure 21 as a function of temperature and pressure (the Mollier diagram in Reference 10 was used to obtain density).

4.4 Three Body Electron Attachment Rate

The attachment time for the three body reaction will be the sum of the dissociation time of the halogen compound and the direct attachment time of Equations 4.12 and 4.1. The elapsed time to reduce the electron concentration to 1/100 its original value is obtained from Equation 4.14 with the second body concentration expressed as density. The expression for t_D^{100} is given below and the values are plotted in Figure 22:

$$t_D^{100} = 2 \times 10^{-12} \rho^{-1} e^{8600/RT} \tag{4.27}$$

The rate of three body electron attachment to fluorine is defined from Equation 4.1 as

$$\frac{d(e)}{dt} = - k_3(F)(e^-)(X) \tag{4.28}$$

The rate coefficient, k_3, obtained from shock time measurements by Good (Ref. 6), is

$$k_3 = 1.5 \times 10^{-37} e^{84,000/RT} \ cc^2\text{-molecule}^{-2}\text{-s}^{-1} \tag{4.29}$$

Integrating Equation 4.28 yields the exponential decay of electron concentration, as follows:

$$(e^-) = (e^-)_o \exp\left[-k_3(F)(X)\, t_3\right] \tag{4.30}$$

The time required to reduce the electron concentration to 1/100 its original value, defined as t_3^{100}, is given as

$$t_3^{100} = \frac{\ell n \frac{(e^-)_o}{(e^-)}}{k_3(F)(X)} = \frac{7 \times 10^{-8} \; e^{-42000/T}}{\chi_F \; \rho^2} \qquad (4.31)$$

The attachment time, t_3^{100}, given in Equation 4.31 has been plotted in Figure 23 as functions of temperature and pressure.

The total attachment time, representing the sum of the dissociation and three body attachment time, is given in Figure 24. At conditions where the dissociation time is short, the attachment time is long and conversely. Consequently, the combined time is always long, and the minimum time is reached at a temperature of 3000°K.

The total attachment time is never less than 10 ms for typical re-entry pressures, and consequently, three body atomic-electron attachment is a mechanism that can only be used in stagnation point regimes. However, its use even at this location is doubtful since the weight requirements to cool the flow to 3000°K may be prohibitive.

5. INJECTION SYSTEM APPLIED TO TRAILBLAZER VEHICLE

The injection system concept will now be carried to specifics and applied to the Trailblazer II vehicle. For purposes of this example, the vehicle's trajectory will be considered a constant velocity flight of 18,000 fps between 125,000 ft. and 300,000 ft. Essentially the vehicle is a blunted sphere-cone having a 6-in. nose radius, a 9° cone angle, and a total vehicle length of 26 in. (Figure 25). The antenna is located near the rear of the vehicle.

The plasma on the Trailblazer II consists of a thin layer with a thickness of about one tenth the nose diameter (Ref. 11). This represents the stagnation point flow that expands around the vehicle nose. The flow field properties, shown in Table III as a function of altitude, were calculated by assuming equilibrium expansion of the flow up to the sonic line. Thereafter, the flow was assumed to be frozen at the sonic conditions and expanded according tc expressions given by Heims (Ref. 12). The pressure is assumed to expand to one tenth the normal shock pressure as indicated by Yakura (Ref. 13) for hypersonic flow over blunted cones.

5.1 Mass Flow Injection Rates

The attachment reaction order and speed will depend on whether the electrophilic gas is injected into a high or low temperature flow. If the electrophilic gas is injected into the stagnation point region, the high temperatures will rapidly dissociate any existing electrophilic molecules thus leaving the atoms to attach electrons by a three body reaction. If the electrophilic gas injected into an expanded flow region where the high temperatures have cooled, the electrophilic molecules will remain intact and will be free to reduce the plasma frequency by dissociative electron attachment.

5.1.1 Three Body Attachment

The three body attachment process is normally quite slow and not useful in alleviating the plasma blackout; however, at high pressures the process is useful. In general, the allowable attachment time is fixed by the flow time of the electrophilic gas between the point of injection and the antenna. Thus, the attachment time is defined as

$$t \leq \int_o^{2.5} \frac{ds}{U} \tag{5.1}$$

where ds is the distance increment along the body. The Trailblazer II body distance from stagnation point to the rear antennas is 2.5 ft.

For three body attachment, the attachment time required to reduce the electron density to one percent of its original value is defined as

$$t_3^{100} = \frac{(t_3^{100}\ \chi_F)}{\chi_F} \tag{5.2}$$

where $(t_3^{100}\ \chi_F)$ is the modified attachment time shown in Figure 23. Substituting Equation 5.2 into 5.1 results in the following attachment time criterion:

$$(t_3^{100}\ \chi_F) < \chi_F \int_o^{2.5} \frac{ds}{U} \tag{5.3}$$

The integral has the value of 2.8×10^{-4} seconds, so that

$$(t_3^{100}\ \chi_F) < 2.8 \times 10^{-4}\ \chi_F$$

Considering for the moment that the upper limit of material addition is

$\chi_F = 0.1$, the modified three body attachment time is

$$(t_3^{100} \chi_F) < 2.8 \times 10^{-5}$$

and as indicated in Figure 23, this is achieved only at pressures above 10^{-2} atm even with the low temperature of T = 2000°K. For the Trailblazer trajectory, three body attachment will only be possible at altitudes below 175,000 ft.

5.1.2 Two Body Attachment

The only reaction which will remove electrons during the entire re-entry trajectory is two body dissociative attachment, and SF_6 is the most effective gas for this since its attachment cross section is the largest known and its equilibrium number of electrons that can be attached is also large. The dissociative attachment will reduce the electron density to at least the equilibrium concentration level of pure air.

To avoid dissociation of SF_6 when it is injected into the plasma, the flow field temperature at the injection point must be less than 3000°K. For all altitudes above 150,000 feet, this can be achieved by injecting at the shoulder; however, at lower altitudes, some SF_6 dissociation must be permitted to cool the plasma so the remaining SF_6 will attach electrons. Details such as this remain to be solved during an actual design. The calculations presented below only illustrate system feasibility.

The amount of SF_6 to be added is determined by three criteria, as mentioned earlier: electron density, attachment rate, and jet momentum. The SF_6 concentration added should be greater than the electron concentration, and for design purposes, the mole fraction of SF_6 added to the plasma should equal 100 times the electron mole fraction, i.e.

$$\chi_{SF_6} = 100\chi_e \qquad (5.4)$$

The mass flow rate is specified as

$$\dot{m} = 100 \ \chi_{el} \ \rho_s \ U_s \ A_P \ \frac{m_{SF_6}}{m_{air}} \tag{5.5}$$

where

ρ_s is the density, lbs/ft^3

U_s is the sonic flow velocity

m_{SF_6} is the molecular weight of SF_6

m_{air} is the molecular weight of air

A_P is the streamtube area containing the plasma passing over the antenna

The effective plasma thickness on a 9° blunted cone is taken as the maximum value tabulated by Russo (Ref. 11) in his Table I for a 9° cone at M = 20 between 60,000 and 230,000 ft. altitude.

$$d_P/D_n \leq 0.144 \tag{5.6}$$

where the nose diameter, D_n, for the Trailblazer II is given as 12 inches. Thus the plasma area, A_P, is defined as the streamtube cross section containing the plasma which affects the antenna. The area is the plasma thickness d_P and the required transmission window width for the Trailblazer II. The cross sectional area at the antenna will thus be essentially

$$A_P = d_P \times w \approx 6 \text{ inches}^2 \tag{5.7}$$

The area of the same streamtube at the point of injection at the shoulder will be three square inches. The required mass flow rate is shown in Figure 26.

Thus the electron density mass flow rate requirement is given as

$$\dot{m} = 1.2 \times 10^{5} \rho_s \chi_{el} = 1.24 \times 10^{-20} N_s \chi_{el} \qquad (5.8)$$

where N_s is the sonic line number density.

The amount of SF_6 required for dissociative attachment of 99 percent of the original electrons within a 2 ft. length is specified as

$$t_2^{100} \leq \int_o^{2.5} \frac{ds}{V} \qquad (5.9)$$

and substituting for the time with Equation 5.2

$$\left(t_2^{100} \chi_{SF_6}\right) \leq 2.8 \times 10^{-4} \chi_{SF_6} \qquad (5.10)$$

and

$$\chi_{SF_6} \geq 3.5 \times 10^{3} \left(t_2^{100} \chi_{SF_6}\right) \qquad (5.11)$$

The mass flow rate of SF_6 that must be injected according to the attachment rate requirement specified by Equation 5.11 is given as

$$\dot{m} = \rho_s U A_P \frac{m_{SF_6}}{m_{air}} \left[3.5 \times 10^{3} \left(t_2^{100} \chi_{SF_6} \right)\right] \qquad (5.12)$$

and substituting the previous values of A_P and $\overline{U}$ and defining weight density,

ρ_s, in terms of the number density, N_s,

$$\dot{m} = 2.2 \times 10^{-26} N_s \left(t_2^{100} \chi_{SF_6} \right) \quad \text{lbs/s} \tag{5.13}$$

For the Trailblazer II conditions given in Table III and Figure 21, the product $N_s(t_2^{100} \chi_{SF_6})$ never exceeds 1×10^{17} $\frac{\text{molecules-s}}{\text{ft}^3}$. Thus the flow rate required for attachment is always less than 10^{-9} lbs/s which is negligible compared to the electron density requirement. Furthermore, the reduction of the electron density to 0.1 percent of its original value would require only a 50 percent increase in time which is still negligible providing equilibrium is not approached.

On the basis of momentum criteria, the mass flow requirements are obtained from Figure 8. The jet centerline penetration distance is defined to be half the plasma layer thickness.

$$\Delta = \frac{1}{2} d_P = 0.9 \text{ inches}$$

The mass flow required to penetrate 0.9 in. into the flow at the shoulder ($M \simeq 2.0$) using a jet Mach No., $M_j = 2$, is found to be

$$\dot{m}_j = 1.1 \times 10^{-2} P_s \quad \text{lbs/s} \tag{5.14}$$

where the jet exit pressure is matched to the local shoulder pressure P_s.

5.2 Reduction of Plasma Attenuation and Reflection

Since mass flow rates are fixed by the jet momentum requirements, there will be more than sufficient time and SF_6 concentration to bring the plasma sheath to equilibrium air conditions within a distance of two feet. Figure 27 illustrates the dramatic alleviation of S-band blackout by the addition of SF_6. The signal attenuation is reduced to zero and the reflection losses reduced to a 3 db peak at 130,000 ft.

5.3 Gas Supply System

The required mass flow rates are shown in Figure 26. The momentum requirements of the Mach 2 jet predominate and determine the mass flow for the Trailblazer II. The total mass required is determined as

$$m_T = \int_{300,000}^{125,000} \dot{m}_j \frac{dh}{U_\infty} = 0.28 \text{ lbs} \qquad (5.15)$$

The SF_6 can be conveniently stored under its own vapor pressure of 310 psig. and the amount of gas that must be stored is determined by the requirement that following expulsion of 0.28 lbs of gas at 125,000 ft, the storage vessel must still have a pressure of $P_{ex} = P_s = 84$ psi. The amount of gas required for isentropic expansion is determined from the following relations:

$$P = \frac{mRT}{V} \qquad (5.16)$$

where

m is the weight of gas in storage

V is the storage volume

T is the gas temperature

R is the gas constant

P is the gas pressure

Differentiating Equation 5.16,

$$\frac{dm}{dt} = \frac{V}{R} \frac{d\left(\frac{P}{T}\right)}{dt} \qquad (5.17)$$

The differential is evaluated from the isentropic relation

$$\left(\frac{P}{P_o}\right) = \left(\frac{T}{T_o}\right)^{\frac{\gamma-1}{\gamma}} \tag{5.18}$$

and substituted into Equation 5.17 to obtain

$$\frac{dm}{dt} = \frac{m}{P}\left[1 - \frac{\gamma-1}{\gamma}\left(\frac{P}{P_o}\right)^{\frac{2(\gamma-1)}{\gamma}}\right]\frac{dP}{dt} \tag{5.19}$$

which is integrated as

$$\ell n\ \frac{m_f}{m_c} = \ell n\ \frac{P_f}{P_o} - \frac{1}{2}\left[\left(\frac{P_f}{P_o}\right)^{\frac{2(\gamma-1)}{\gamma}} - 1\right] \tag{5.20}$$

With the requirements that P_o equal 300 psia, P_f equal 84 psia, and γ equal 1.09, the ratio of final to initial mass weight of SF_6 stored in the vessel is found to be

$$\frac{m_f}{m_o} = .31$$

and the expelled weight is defined as

$$m_o - m_f = 0.28 \text{ lbs} .$$

Thus the initial stored weight is determined to be

$$m_o = 0.4 \text{ lbs.}$$

The 0.4 lbs of SF_6 required for the Trailblazer II flight test is a representative value. Optimization is required on the orifice size, jet Mach No. and gas weights to cover the wide range of exit pressures required for a correctly expanded jet.

The density of the SF_6 stored as a liquid under its own vapor pressure at $70^{\circ}F$, is 3.25 lbs/ft^3, and the storage vessel size required for 0.4 lb of SF_6 is 0.124 ft^3 or 215 in^3 with a 3.7 in. radius. A spherical vessel of this size made of 4340 steel with a burst pressure of 900 psi would weigh 1.5 lbs, and the regulator, fill valves, on-off switches, squib valves, and required plumbing would add another 1.5 lbs to the system (Ref. 15). Thus the total system would weigh 3.4 lbs when charged with SF_6.

The system parameters that have been specified illustrate the feasibility of alleviating radio communication blackout. This is by no means the optimum or desired system for a flight test. The specific program may have smaller volume available. In which case, the amount of mass and storage volume can be reduced by pulsing the gas jet.

5.4 Jet Effect on Vehicle Aerodynamics

The use of a side jet to create an electromagnetic window will create a moment, upsetting the vehicle trim. The trim angle can be obtained by balancing the jet moment with the aerodynamic moment produced by the trim angle.

$$N_j \ell = C_{N_\alpha} \frac{\rho_\infty V_\infty^2}{2} \frac{\pi D^2}{4} \alpha_{trim} \bar{x}$$

where

N_j is the jet normal force

ℓ is the axial distance between the jet and the center-of-pressure.

D is the vehicle base diameter

C_{N_α} is the normal

α_{trim} is the trim angle

$\bar{x}$ is the static margin

For the Trailblazer II vehicle

ℓ = 5.4 inches

C_{N_α} = .015 per degree

D = 20 inches

$\bar{x}$ = 0.54 inches

The jet normal force is assumed to be twice the jet exit momentum

$$N_j = 2\dot{m}U_j$$

For the Mach 2 jet assuming a gas storage temperature of 520°R,

$$N_j = 50.5\,\dot{m} \quad \text{lbs}$$

Thus the trim angle can be evaluated as a function of altitude using the following relation

$$\alpha_{trim} = 214\,\frac{\dot{m}}{\rho_\infty V_\infty^2}$$

For the mass flow rates specified in Figure 27, the trim angle is calculated to be about 0.35 degrees down to 180 km and hereafter increases to 0.6 degrees at 125 km.

Such a value for the trim angle of attack is not considered a problem.

6. CONCLUSIONS

The use of a high heat capacity gas to cool the plasma and create a radio communications window was shown to have no effect on the plasma frequency or electron density. The use of such a gas, however, does cool the plasma temperature but has no effect on the electron recombination rates which remain too slow to appreciably reduce the electron density near the point of gas injection. Numerical calculations at T = 5075°K and P = 0.1 atm indicate that equilibrium cooling of electrons would require a distance of about ten meters.

Speedy removal of electrons can only be achieved by adding material to react with the electrons to form new, fast recombination mechanisms. Halogens are particularly useful for this and the electrophilic gas, SF_6, has the largest known electron attachment cross section. Thus, SF_6 added to the plasma will rapidly remove electrons in a two body process known as dissociative attachment. Studies to determine conditions where dissociative attachment would occur showed that if the SF_6 is injected into a plasma which has cooled by expansion to temperatures below 3000°K, the SF_6 molecule will remain intact until it encounters a free electron. Typical attachment times for re-entry plasma conditions are less than ten microseconds for ten percent mole fraction of SF_6 added.

A SF_6 gas injection system for the Trailblazer II has been studied and demonstrated feasible. The preliminary design developed during this study indicates that a system weighing 3.4 pounds is all that is required to reduce the S-band attenuation and reflection to essentially zero throughout the re-entry. A detailed design is now required to develop the actual mechanical design of the storage vessel, regulator, nozzle and associated plumbing. For the Trailblazer II vehicle it appears feasible that the SF_6 can be stored as a liquid under its own vapor pressure in tubing wrapped around inside the vehicle base. Thus the gas injection system can be designed and installed which will not affect the payload carried.

REFERENCES

1. Adams, R. H. and Rossi, J. J., Research of Aerodynamic Methods of Producing Antenna Windows in a Plasma Sheath, MITHRAS, Inc., Report No. MC 63-78-R1, October 1964.

2. Ricou, F.P. and Spalding, D.B., "Measurement of Entrainment by Axisymmetric Turbulent Jets," J. Fluid Mechanics, Vol 11, Part 1, August 1961.

3. Vinson, Paul W., "Extension of Reaction Control Effectiveness Criteria to Mach 10; Experiment and Theory," AIAA, Vol. 3, No. 10, p. 536 (1965).

4. Abramovich, G.N., The Theory of Turbulent Jets, MIT Press, 1963.

5. Vincenti, Walter G., Calculations of the One-Dimensional Non-Equilibrium Flow of Air Through a Hypersonic Nozzle, AEDC TN 61-55 (1961).

6. Good, R. Earl, Electron Attachment to Atomic Fluorine in Thermally Ionized Air, MITHRAS, Inc., Report No. MC 64-82-R1, June 1965.

7. Jacobs, T.A. and Giedt, R.R., "Dissociation of Cl_2 in Shock Wave," J. Chemical Physics, Vol. 39, 749, August 1963.

8. Modica, A.P. and LaGraff, J.E., Shocktube Kinetic Studies of the Tetrafluorethylene-Oxygen System, Avco Corp., Report RAD-TM-63-29 (1965).

9. Buchel'nikova, I.S., "Cross Sections for the Capture of Slow Electrons by O_2 and H_2O Molecules and Molecules of Halogen Compounds," JETP 35, No. 5, May 1959.

10. Moechel, W.E. and Weston, K.C., Composition and Thermodynamic Properties of Air in Chemical Equilibrium, NASA TN 4265, April 1958.

11. Russo, Anthony, J., Estimates of Attenuation and Reflection of Telemetering Signals by Ionized Flow Fields Surrounding Typical Re-entry Bodies, NASA TN D-1778, 1963.

12. Heims, Steve P., Effects of Chemical Dissociation and Molecular Vibrations on Steady One-Dimensional Flow, NASA TN D-87, August 1959.

13. Yakura, James K., A Theory of Entropy Layers and Nose Bluntness in Hypersonic Flow, ARS Preprint No. 1983-61.

14. Treanor, C.E. and Logan, J.G. Jr., Tables of Thermodynamic Properties of Air from 3000°K to 10,000°K, Cornell Aeronautical Laboratory Report No. AD-1052-A-2, 1956.

15. Good, R. Earl, Aerodynamic Gas Spike Antenna for Re-Entry Propagation Flight Test (U), MITHRAS, Inc., Report No. MC 63-79-R2 (Confidential), 1964.

16. Mahan, Bruce, H. and Young, Charles E. "Gaseous Thermal Electron Reactions: Attachment to SF_6 and C_7F_{14}." J. Chem. Phys. 44, 2192 (1966).

TABLE I

PROPERTIES OF ELECTROPHILIC GASES

Species	Energy Level n	Electronic Degeneracy g_n	Electronic Energy ϵ_n, ev	Ionization Energy ev	Electron Affinity ev
F	0	4	0	17.418	-3.63
	1	2	12.71		
Cl	0	4	0	13.01	-3.78
	1	2	0.109		
	2	1	8.825		
Br	0	4	0	11.84	-3.54
I	0	4	0	10.454	-3.24
O	1	5	0	13.614	-1.0
	2	3	1.967		
SF_6					0
CF_3				10.1	- .9
H_2O				9.511	
S				10.357	-2.5
C				11.256	-1.13

TABLE II

PROPERTIES OF SF_6 AND CF_4

Specie	Molecular Weight g/mole M	Specific Heat cal/mole-°c C_P	Enthalpy at 300°K cal/mole H_{300}	Bond Energy k/cal/mole ΔE	ΔH Dissociation kcal/mole
SF_6	146.06	23.22	6945	85	426
SF_5	127.06	4R	----	65	---
SF_4	108.06	4R	----	65	---
SF_3	89.06	4R	----	65	---
SF_2	70.06	4R	----	65	---
SF	51.06	7/2R	----	65	---
S	32.06	5.66	----	--	---
F	.19	5.436	----	--	---
CF_4	88.01	4R	5992	123	462
CF_3	69.01	4R	----	113	---
CF_2	50.01	4R	----	113	---
CF	31.01	7/2	----	113	---
C	12.01	4.98	----	--	---

TABLE III

TRAILBLAZER II FLOW FIELD PARAMETERS

Elapsed Time	Altitude	P_2	T_2	P_s	T_s	P_A	T_A	χ_{el_2}	$t_2^{100}\chi_{SF_6}$	N_s
		Normal Shock		Equilibrium Sonic		Frozen Expansion			Seconds	$mole/ft^3$
seconds	feet	atm	^oK	atm	^oK	atm	^oK			
0	300,000	4.75 -4	3920	2.8-4	3700	5-5	2100	3.1-5	3.5-5	1.2+ 19
1.39	275,000	1.925-3	3830	1-3	3500	2-4	2060	1.8-5	1-5	4.6+ 19
2.78	250,000	7.65 -3	4140	5-3	3800	7-4	2100	1.4-5	3-6	2.1+ 20
4.17	225,000	2.15 -2	4050	1.1-2	3600	2-3	2130	1-5	1-6	4.9+ 20
5.56	200,000	5.37 -2	4070	2.6-2	3600	5-3	2190	8-6	4-7	1.2+ 21
6.95	175,000	1.925-1	4240	7-2	3800	1.4-2	2300	2-6	1.6-7	2.8+ 21
8.34	150,000	4.17 -1	4780	2.3-1	4300	4-2	2500	2-5	1.4-7	8.0+ 21
9.73	125,000	1.356	5880	8-1	5500	1.4-1	3100	1-4	8-8	2.9+ 22

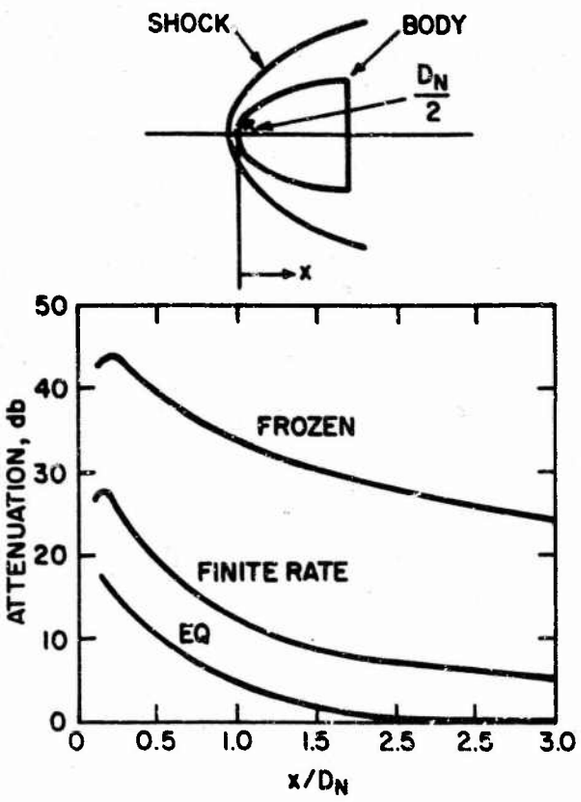

Figure 1. Radio Attenuation Around a Blunt-Body Vehicle

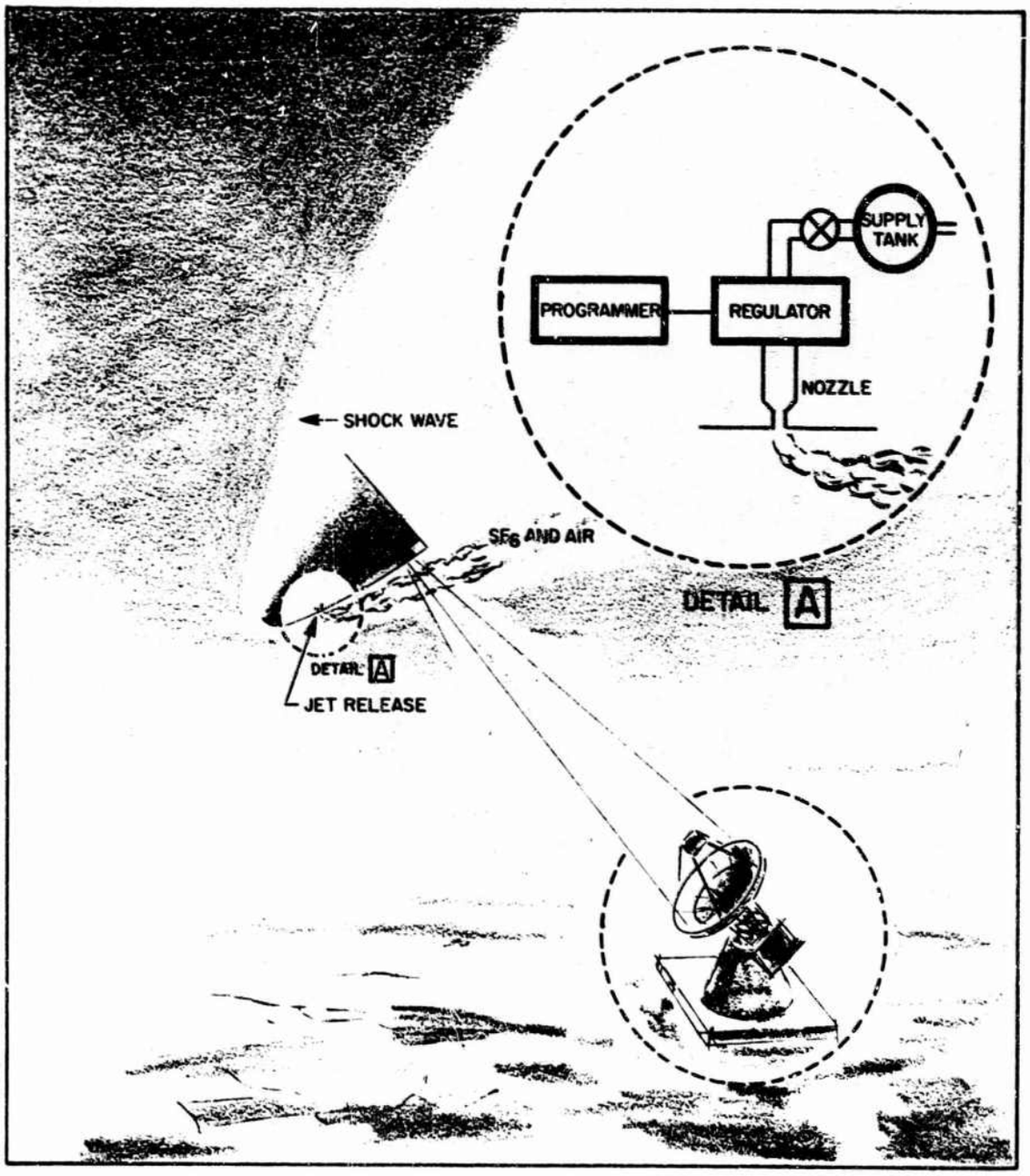

Figure 2. Schematic of Injection System

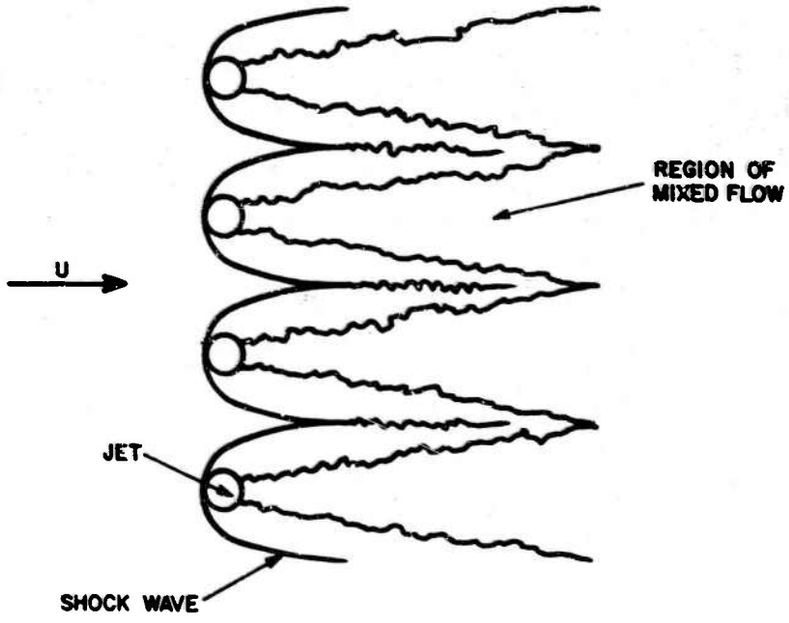

Figure 3. Plan View of Jet Injection System

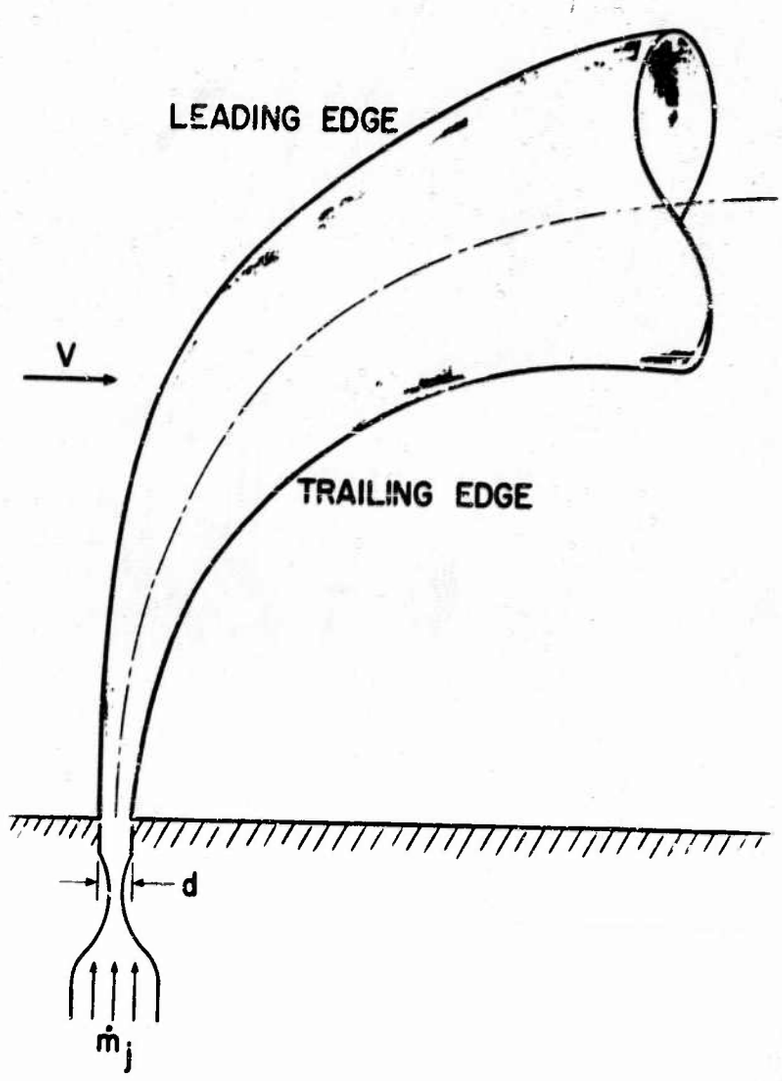

Figure 4. Circular Cross Jet in a Supersonic Free Stream

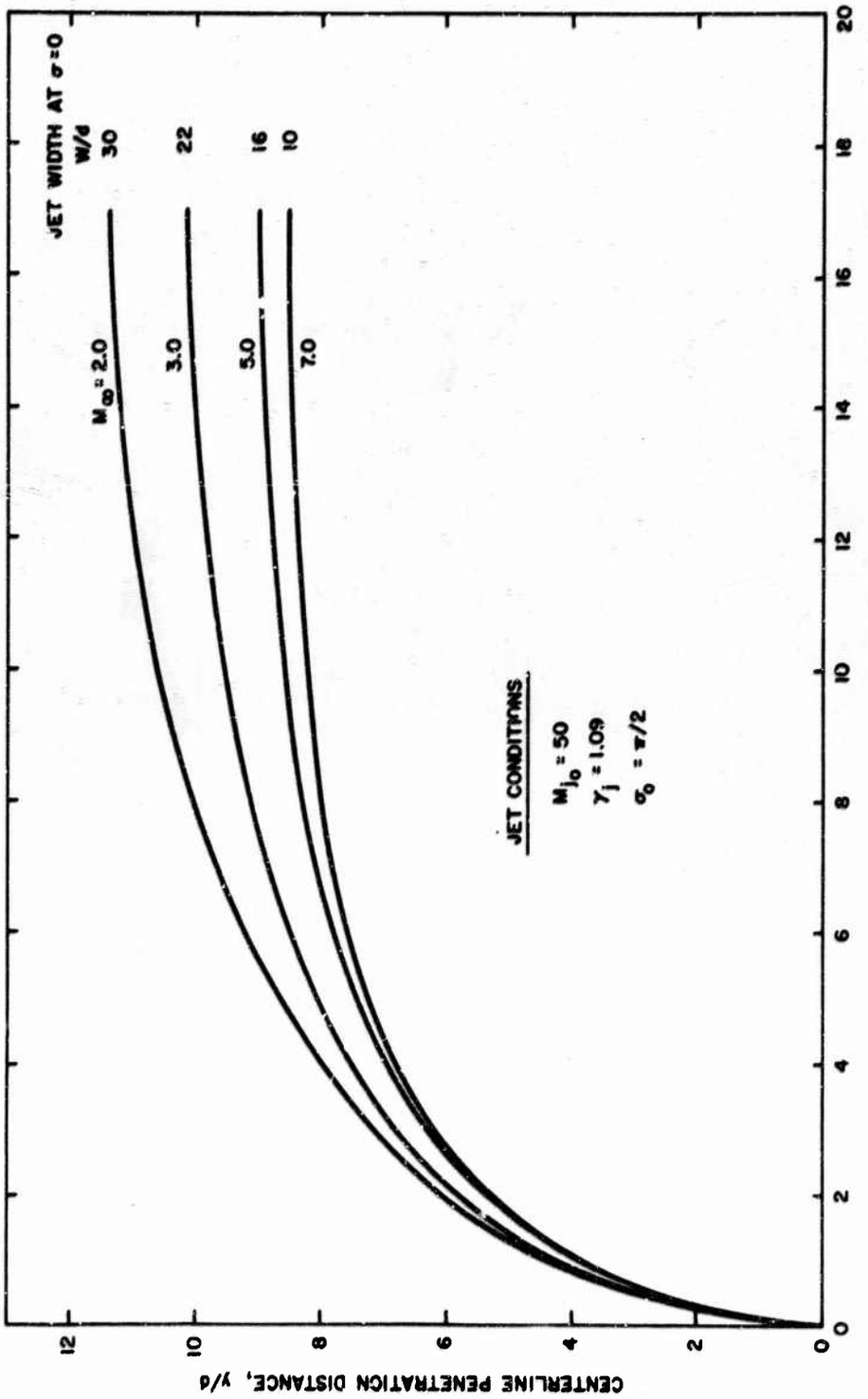

Figure 5. Centerline Penetration Distances

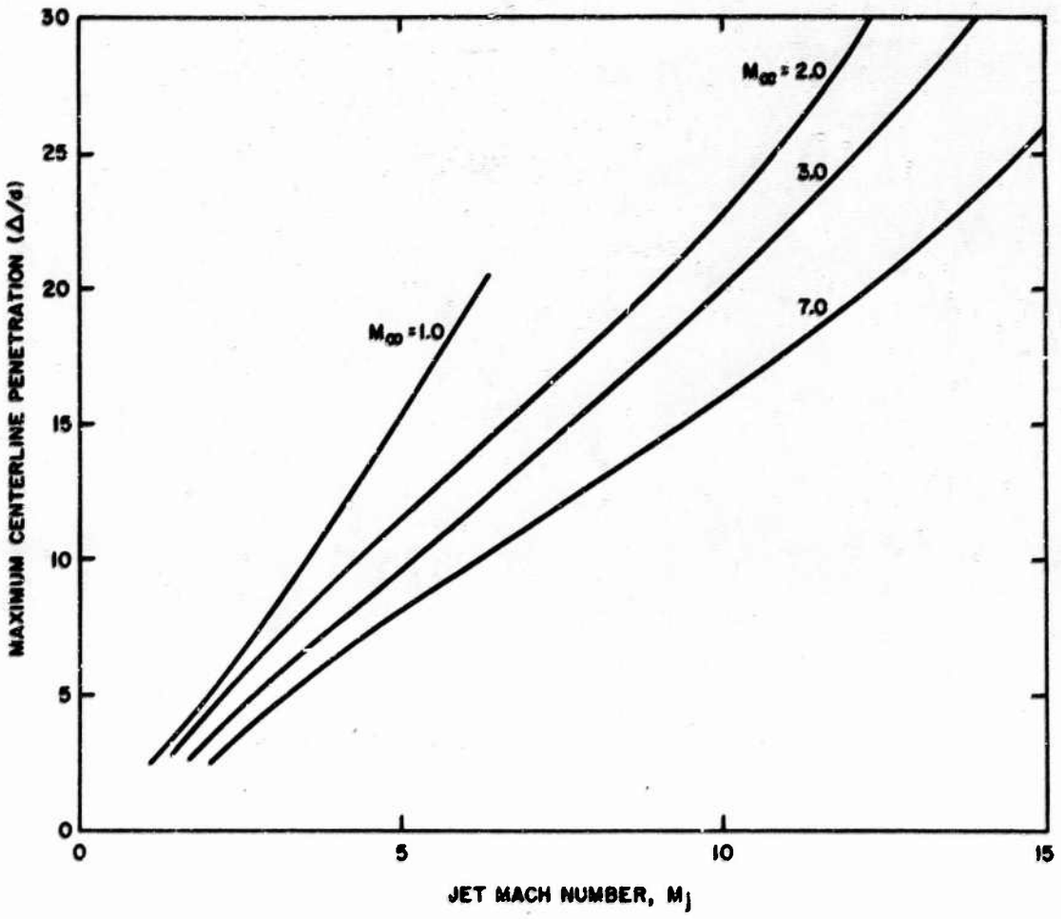

Figure 6. Effect of Jet Mach Number on Penetration Distance

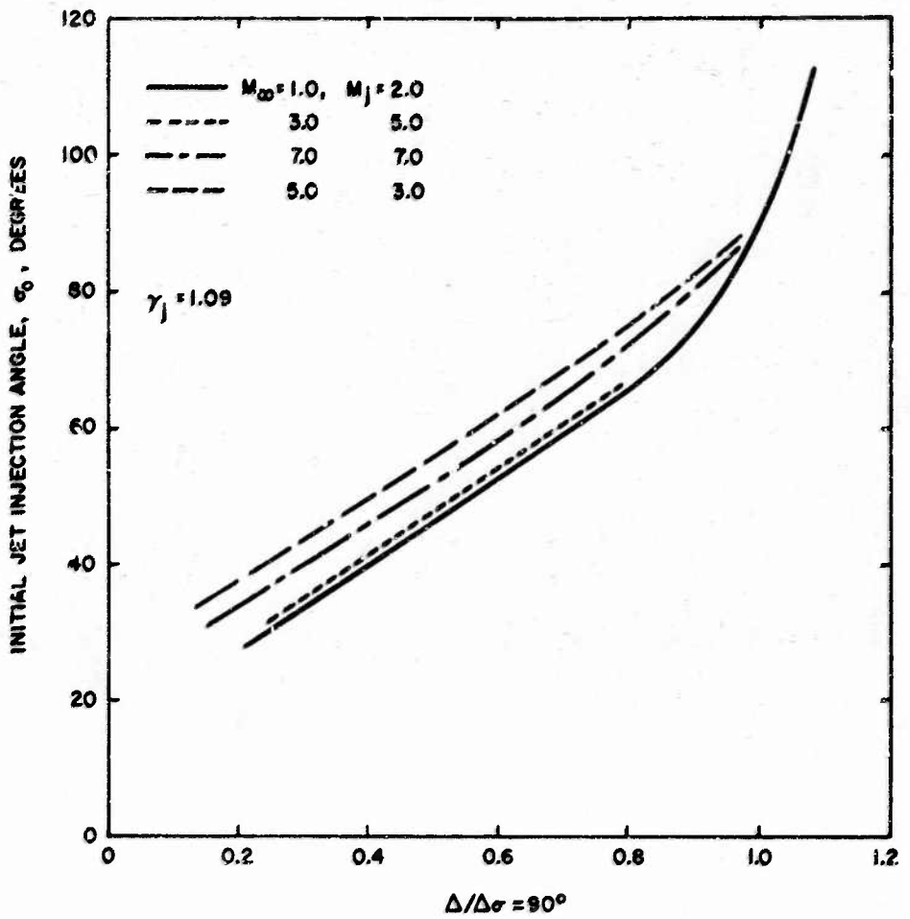

Figure 7. Effect of Jet Injection Angle on Penetration Distance

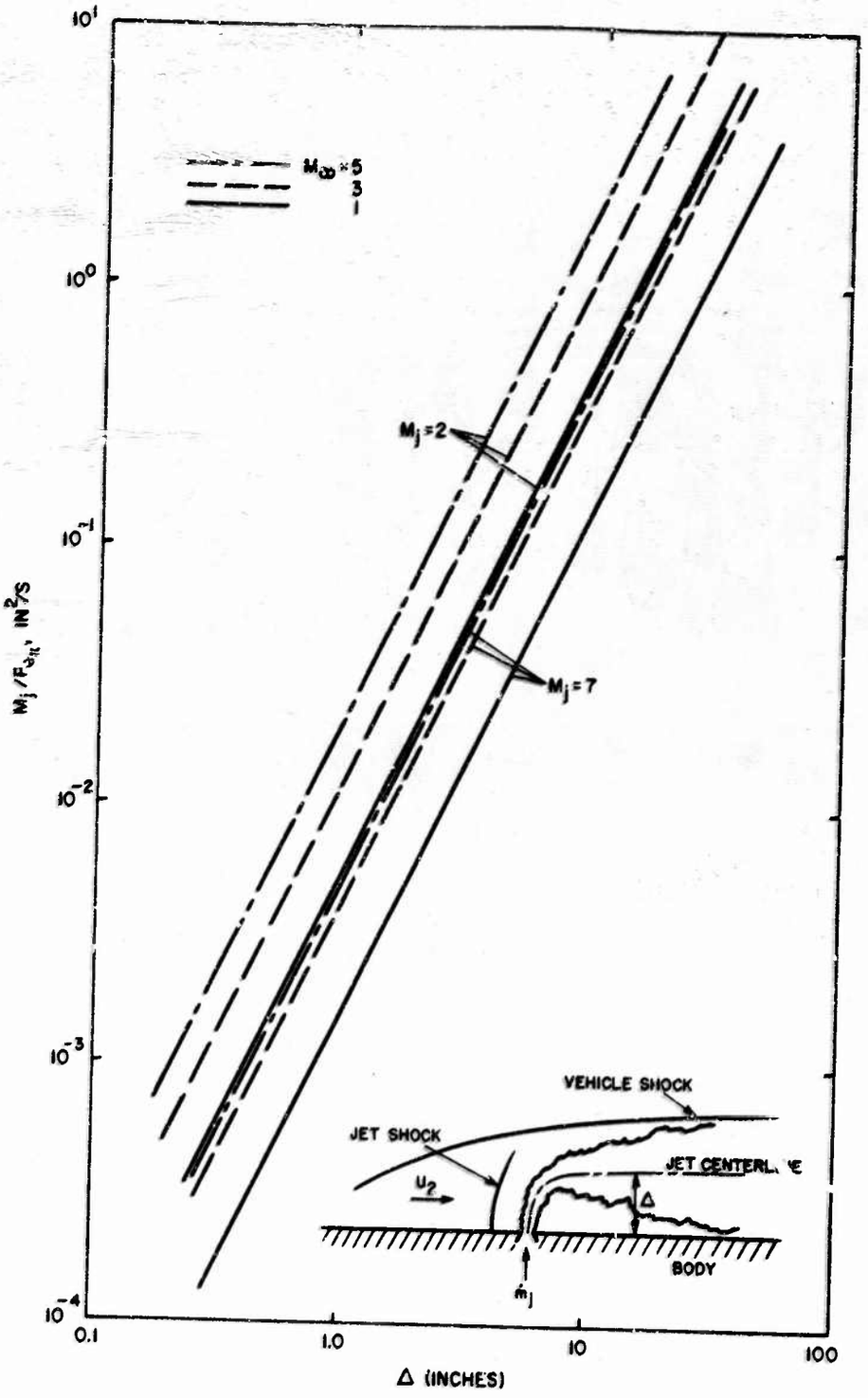

Figure 8. Jet Mass Flow Requirements for Injection of SF_6

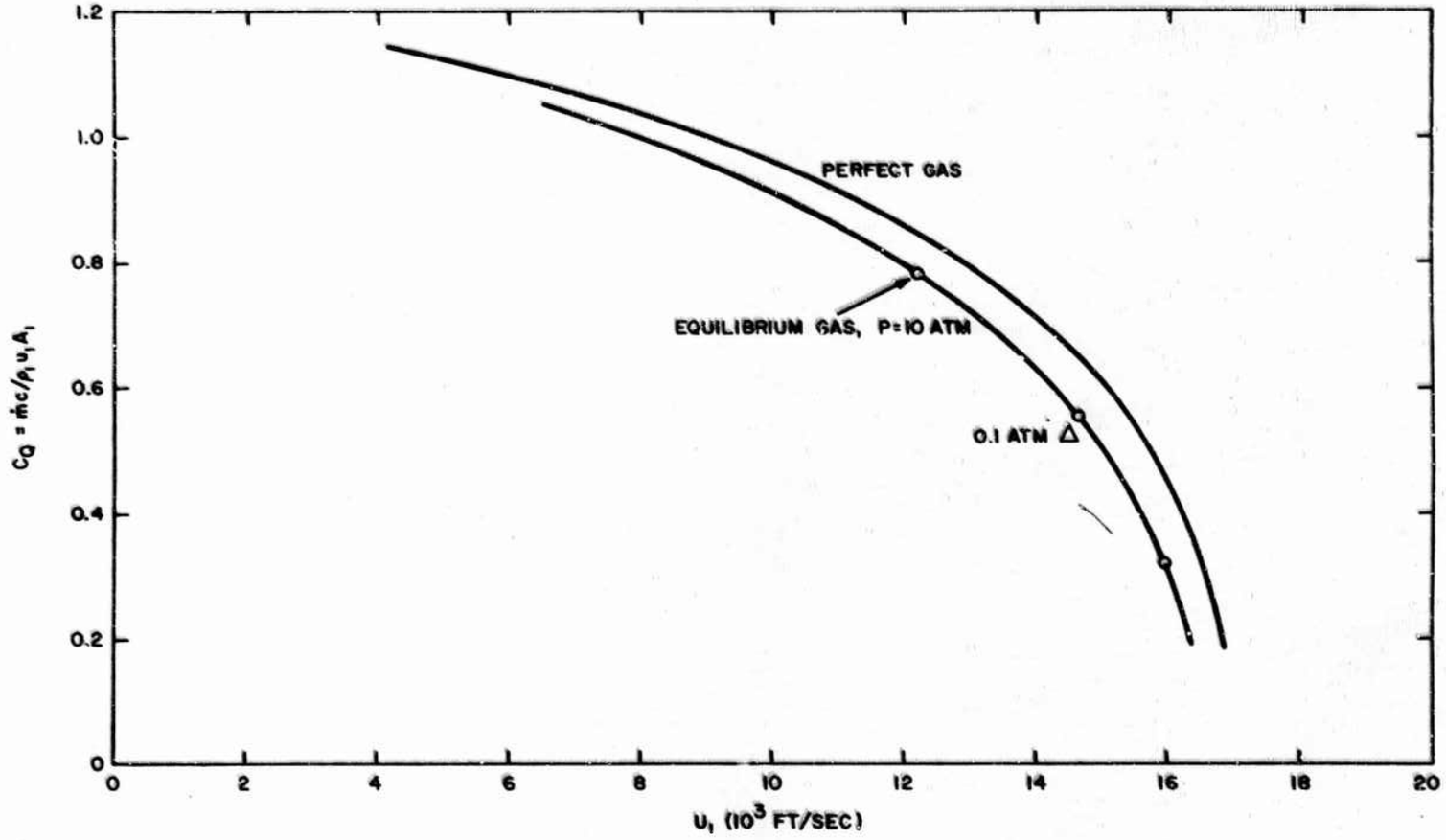

Figure 9. Mass Flow Requirements to Cool Plasma to 2400°K

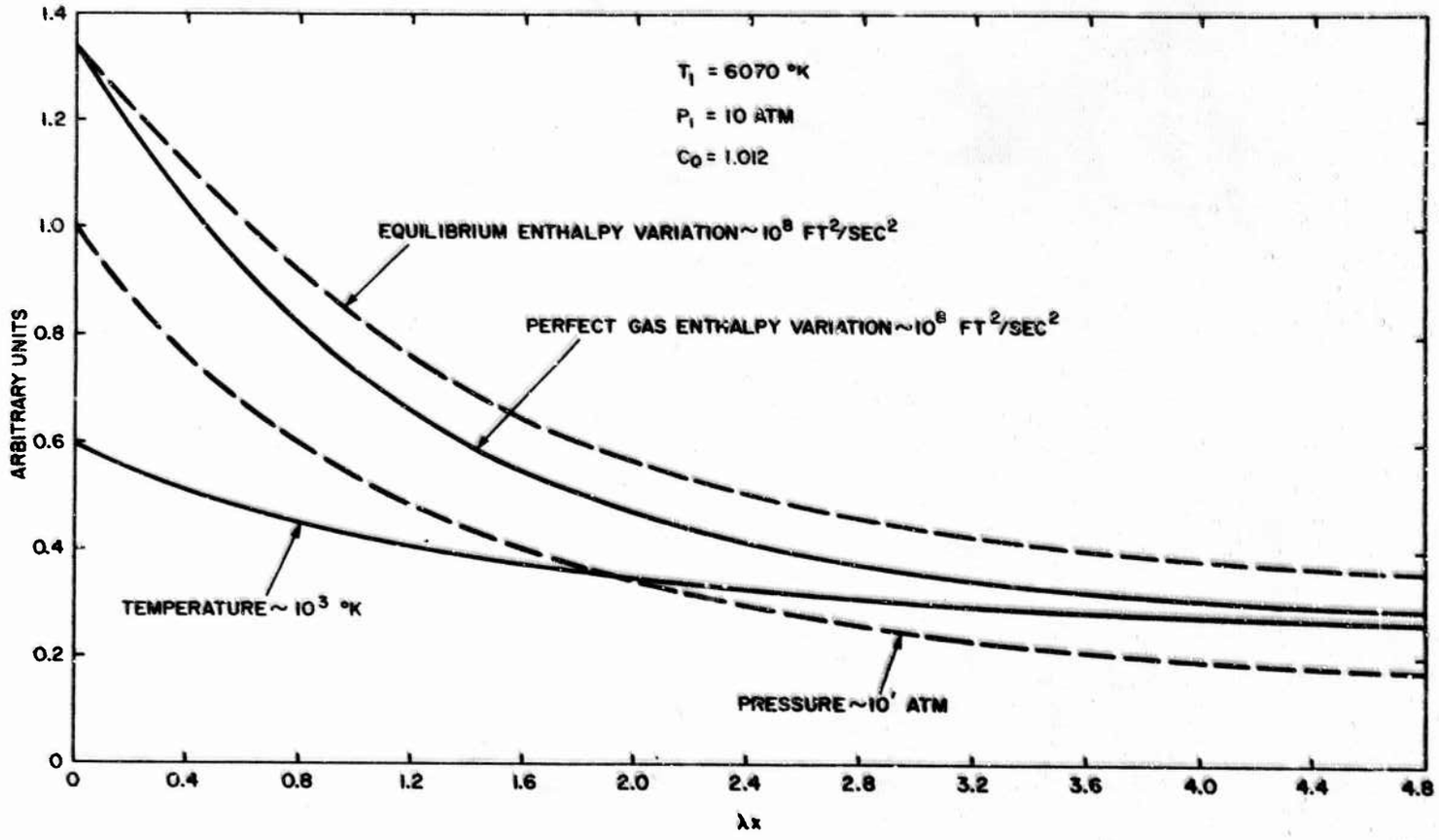

Figure 10. Estimate of Equilibrium Gas Variation of Temperature, Pressure, and Enthalpy

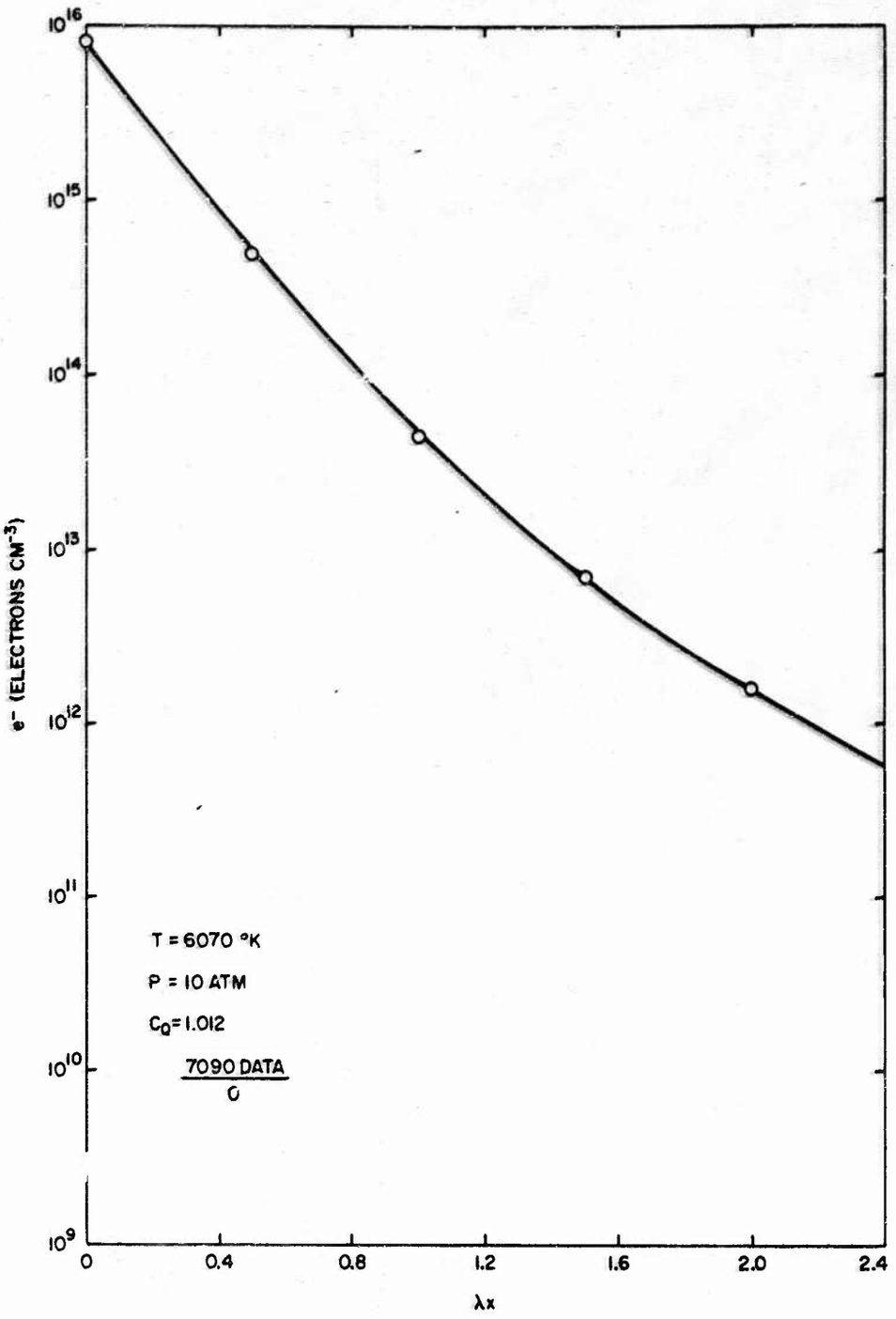

Figure 11. Equilibrium Change in Electron Density with Distance

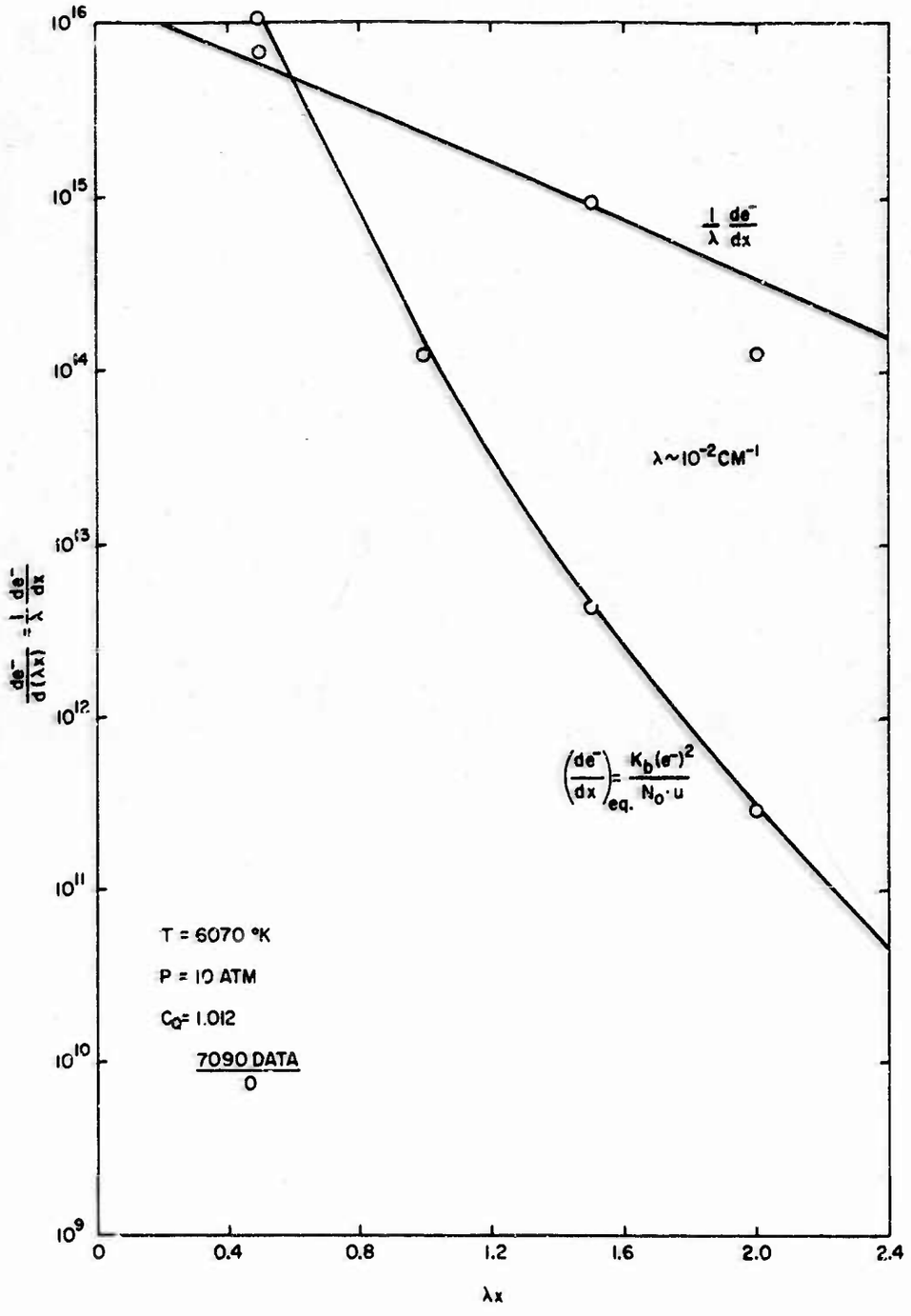

Figure 12. Comparison of Cooling and Electron Recombination Rates

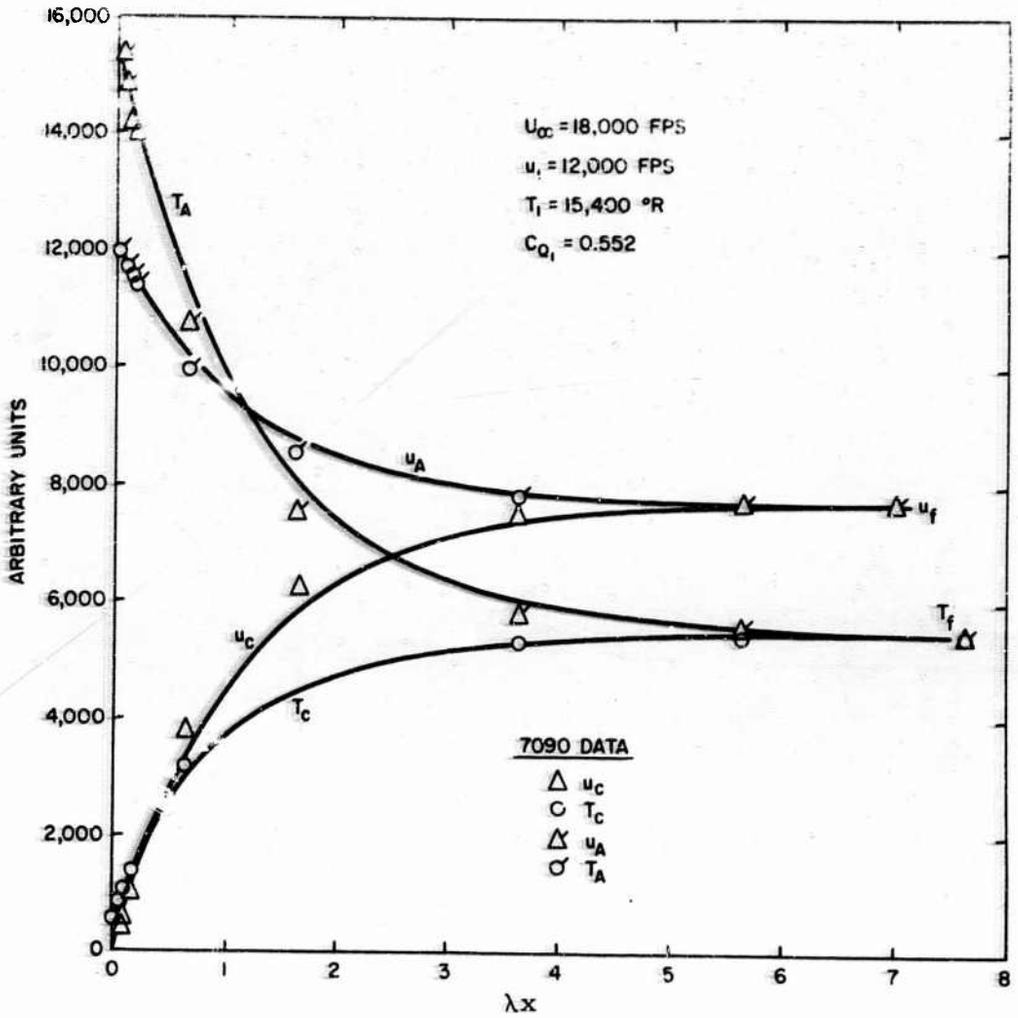

Figure 13. Perfect Gas Cooling

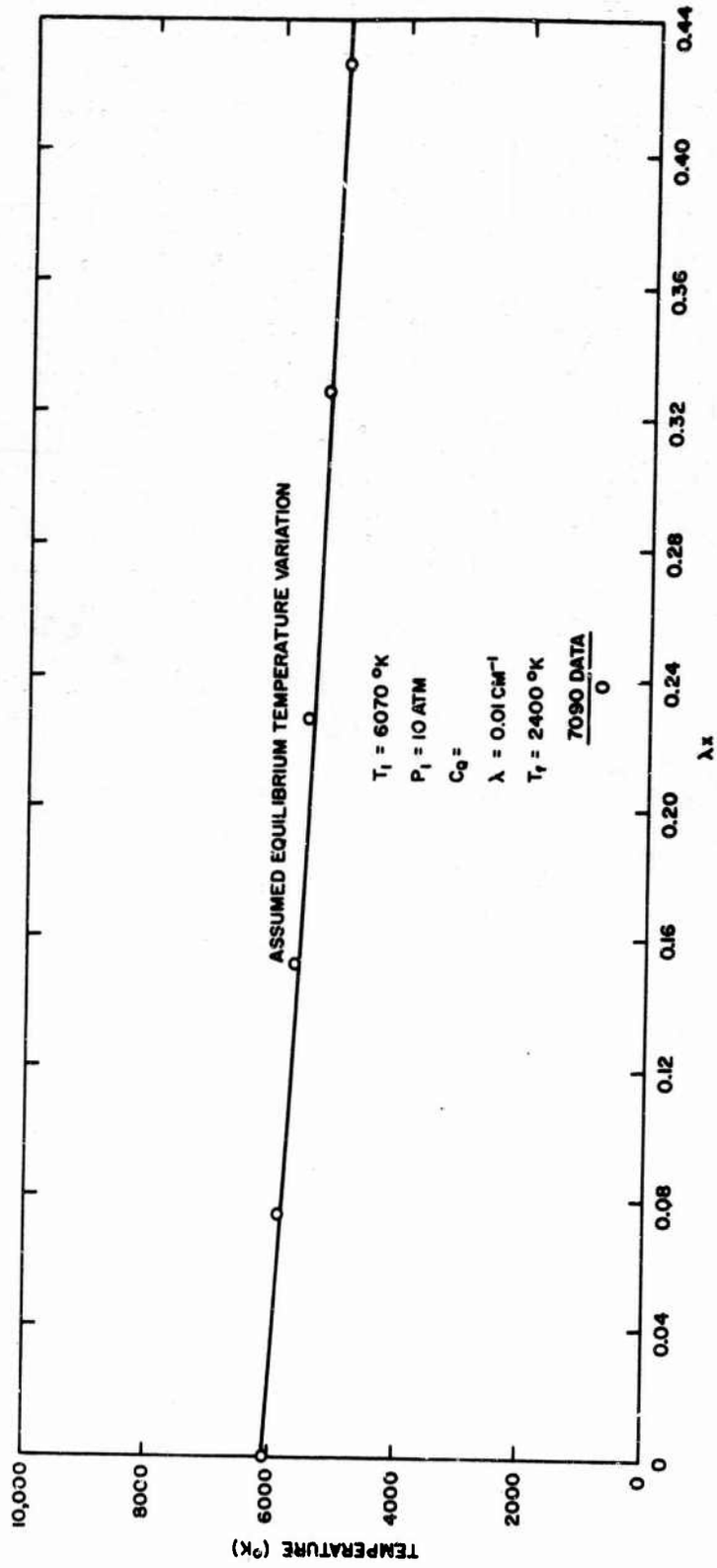

Figure 14. Equilibrium Gas Cooling

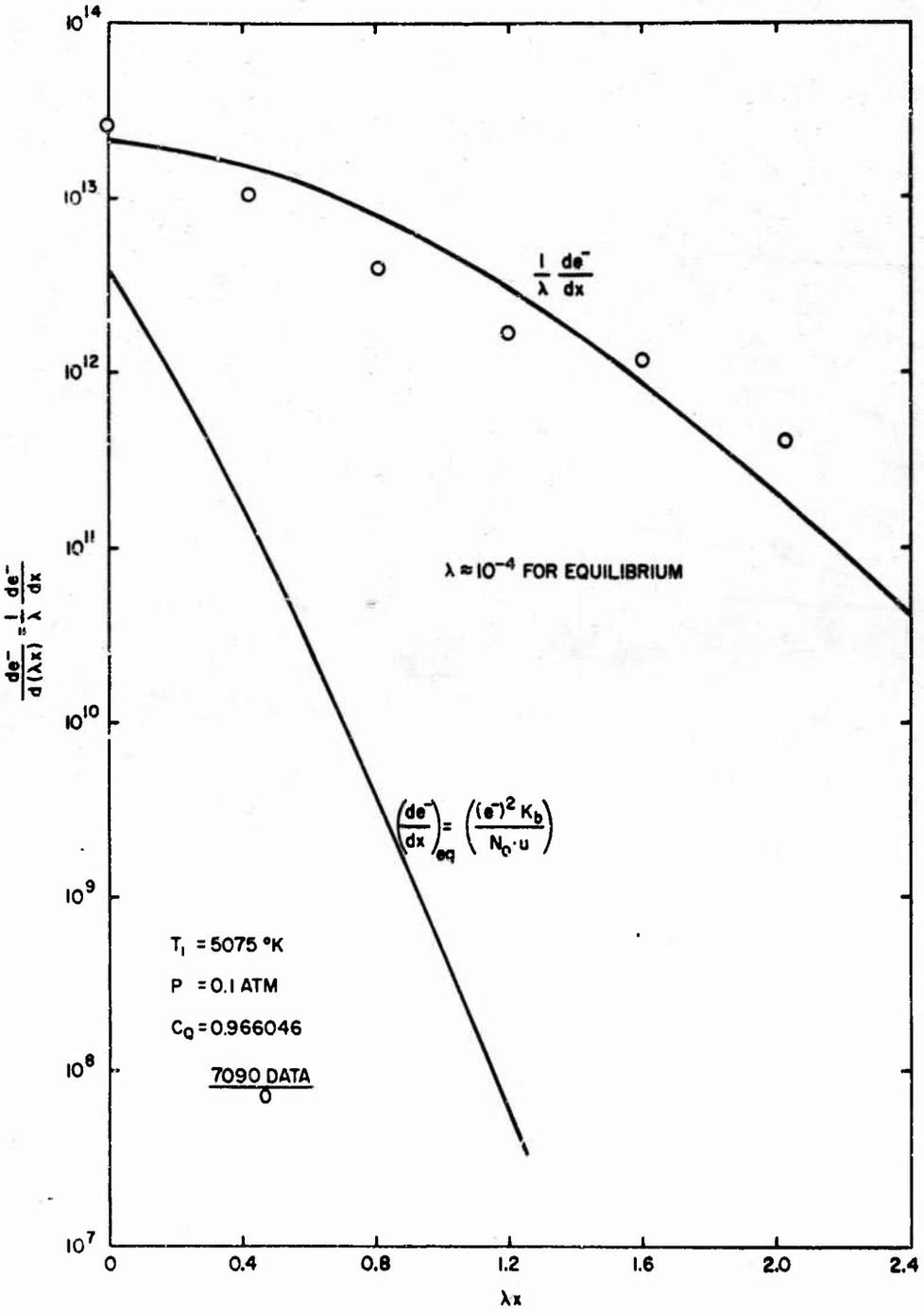

Figure 15. Frozen Gas Cooling

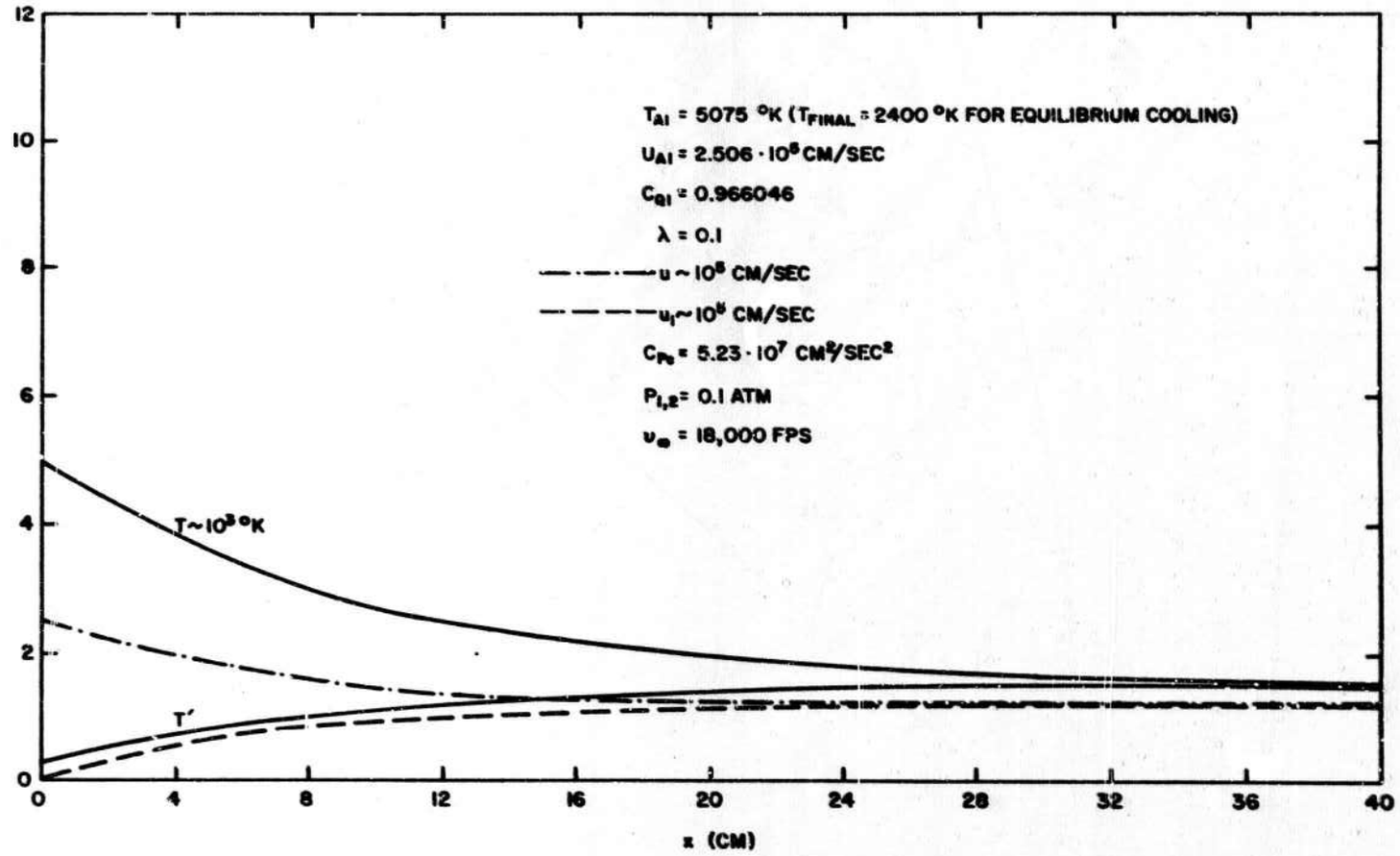

Figure 16. Temperature and Velocity During Frozen Flow Cooling

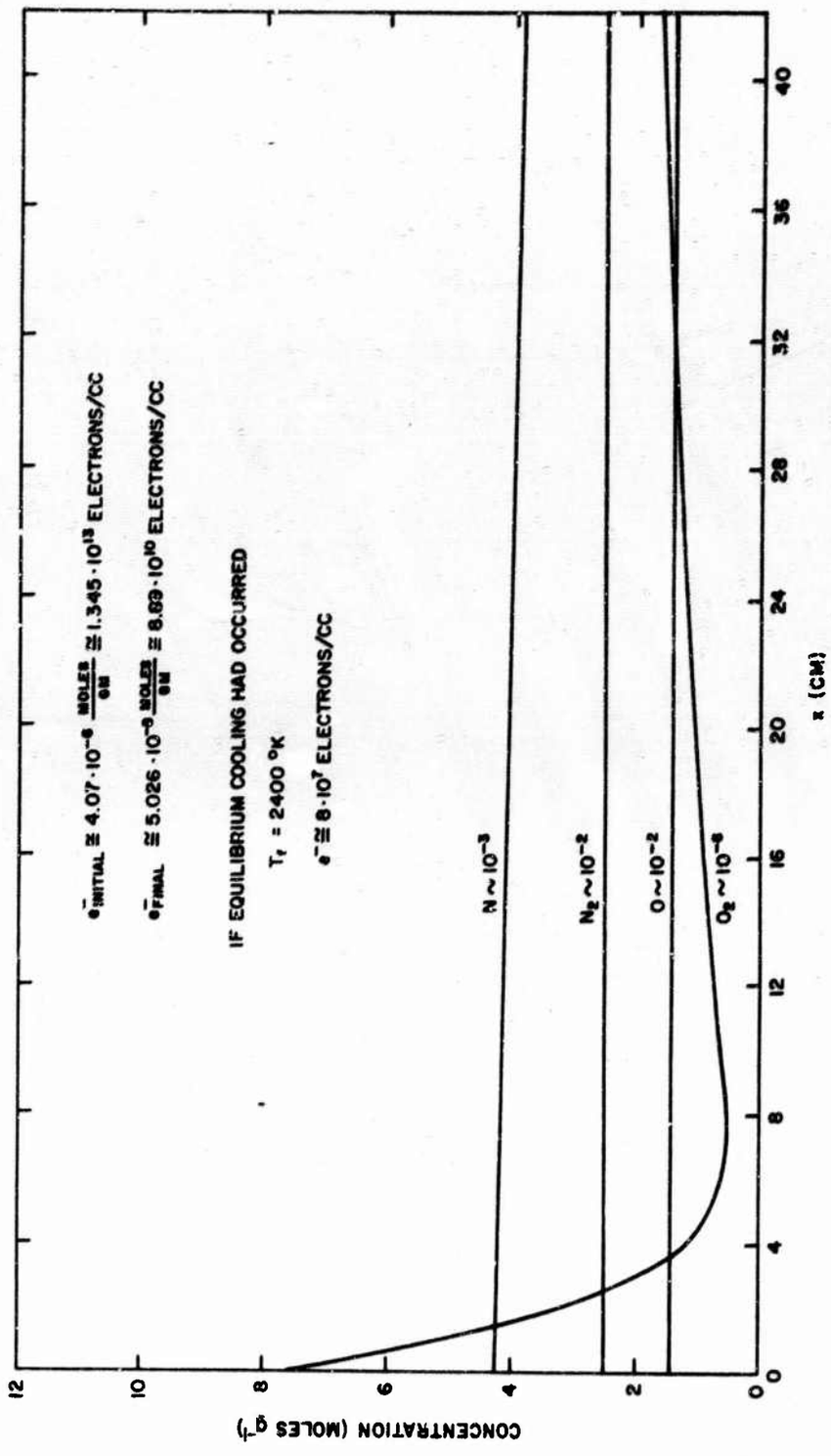

Figure 17. Specie Concentration During Frozen Flow Cooling

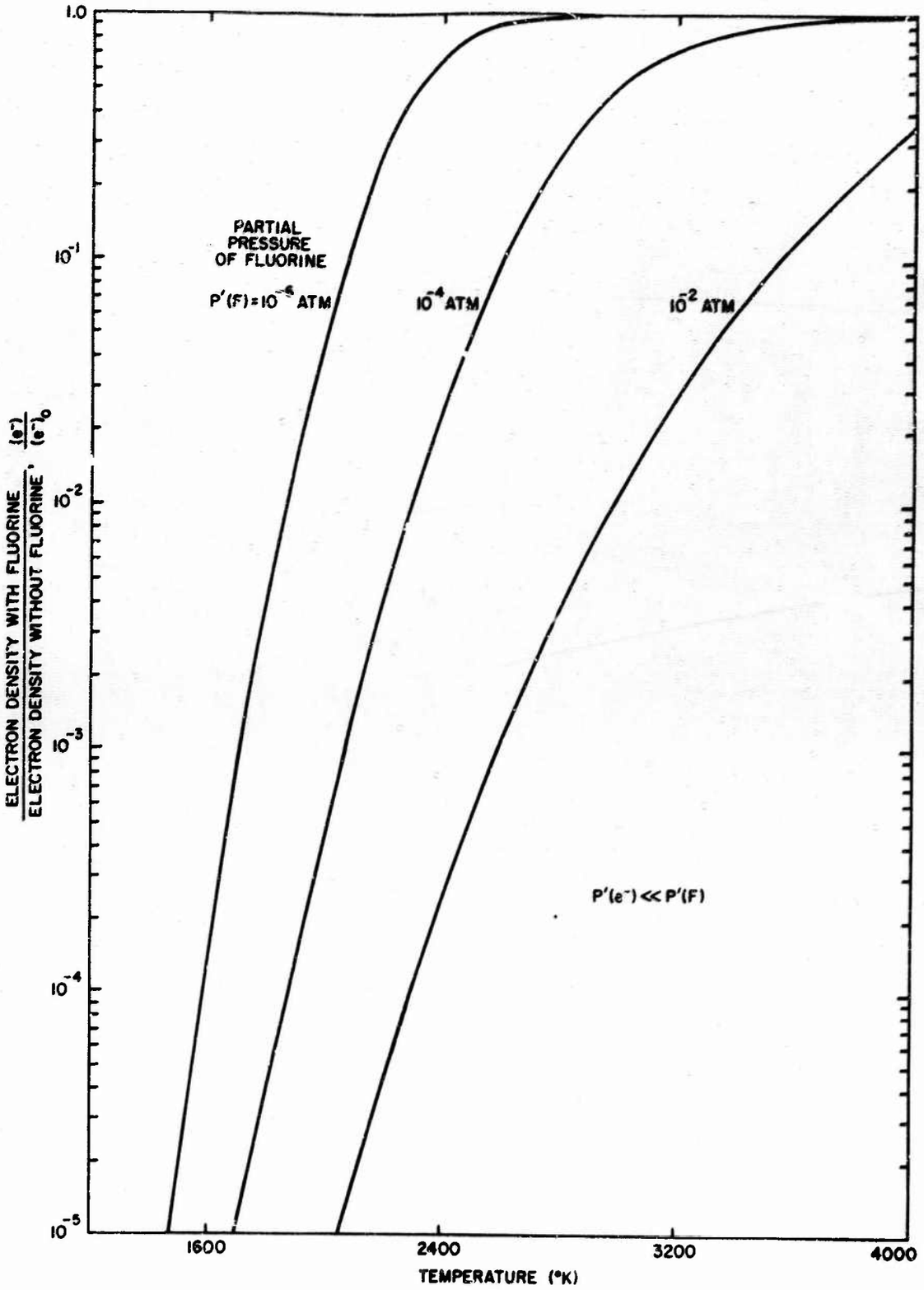

Figure 18. Equilibrium Electron Density with Attachment

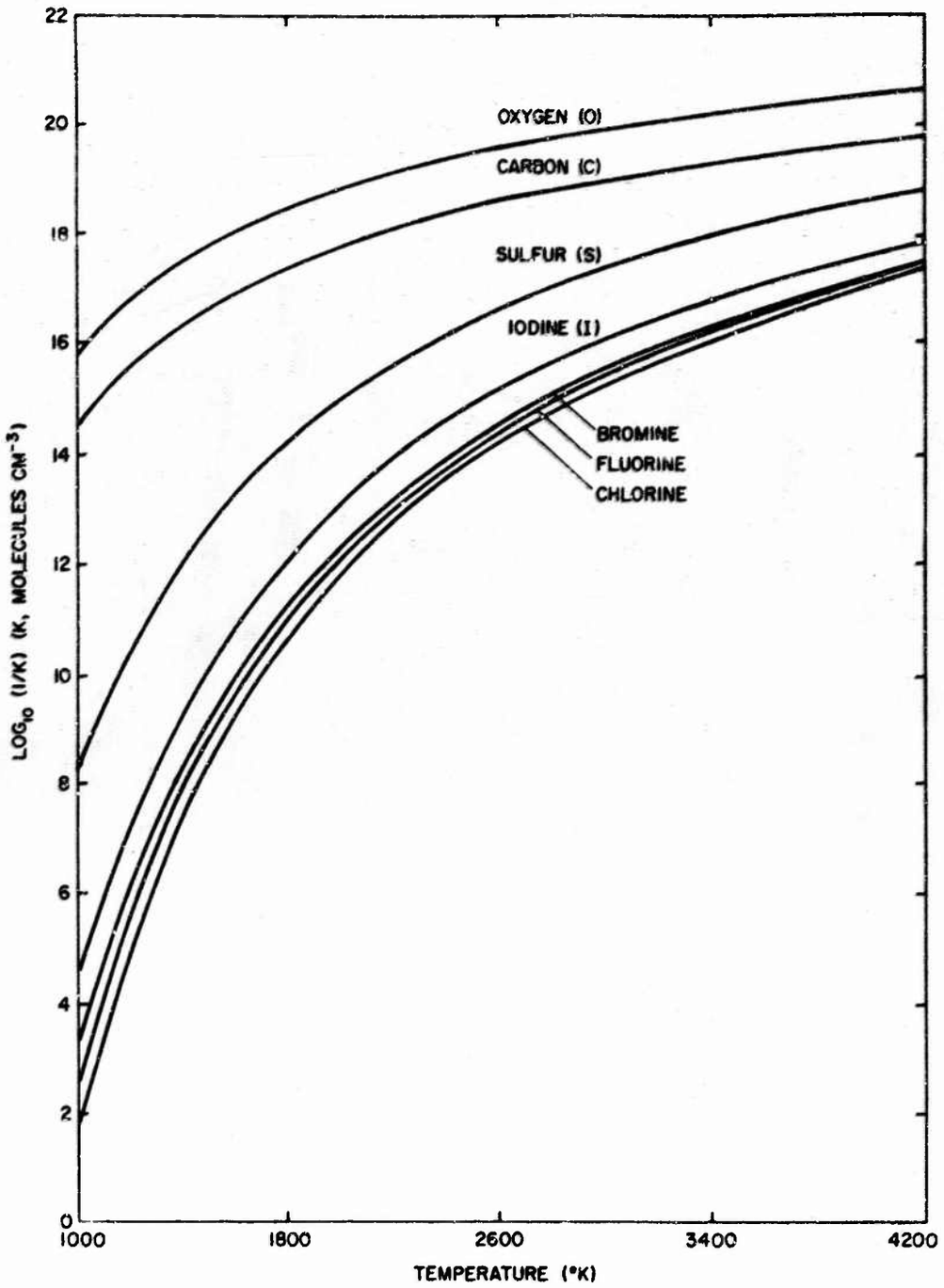

Figure 19. Equilibrium Constants for Electron Attachment to Atoms

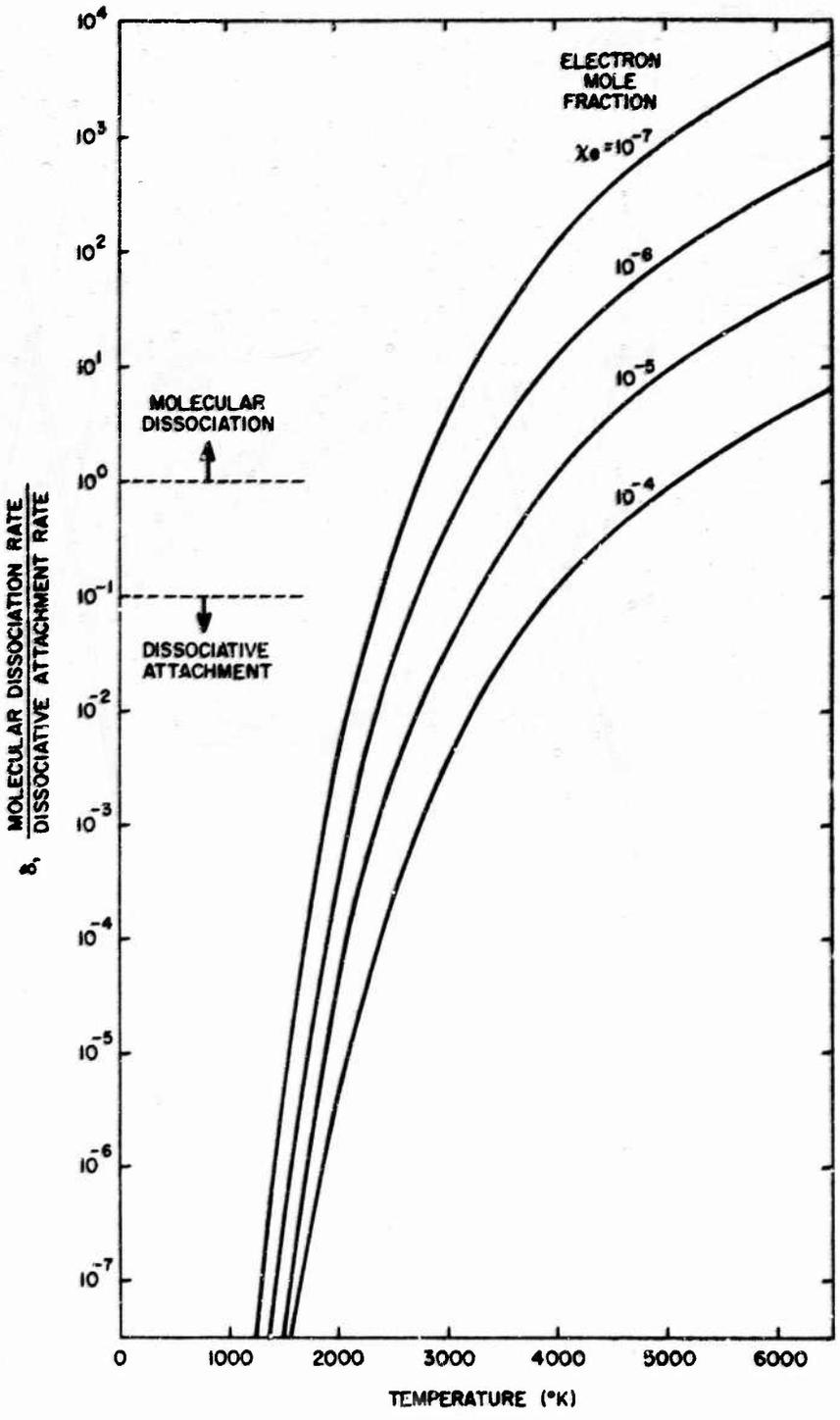

Figure 20. Relative Importance of Molecular and Electron Collisions in SF_6 Dissociation

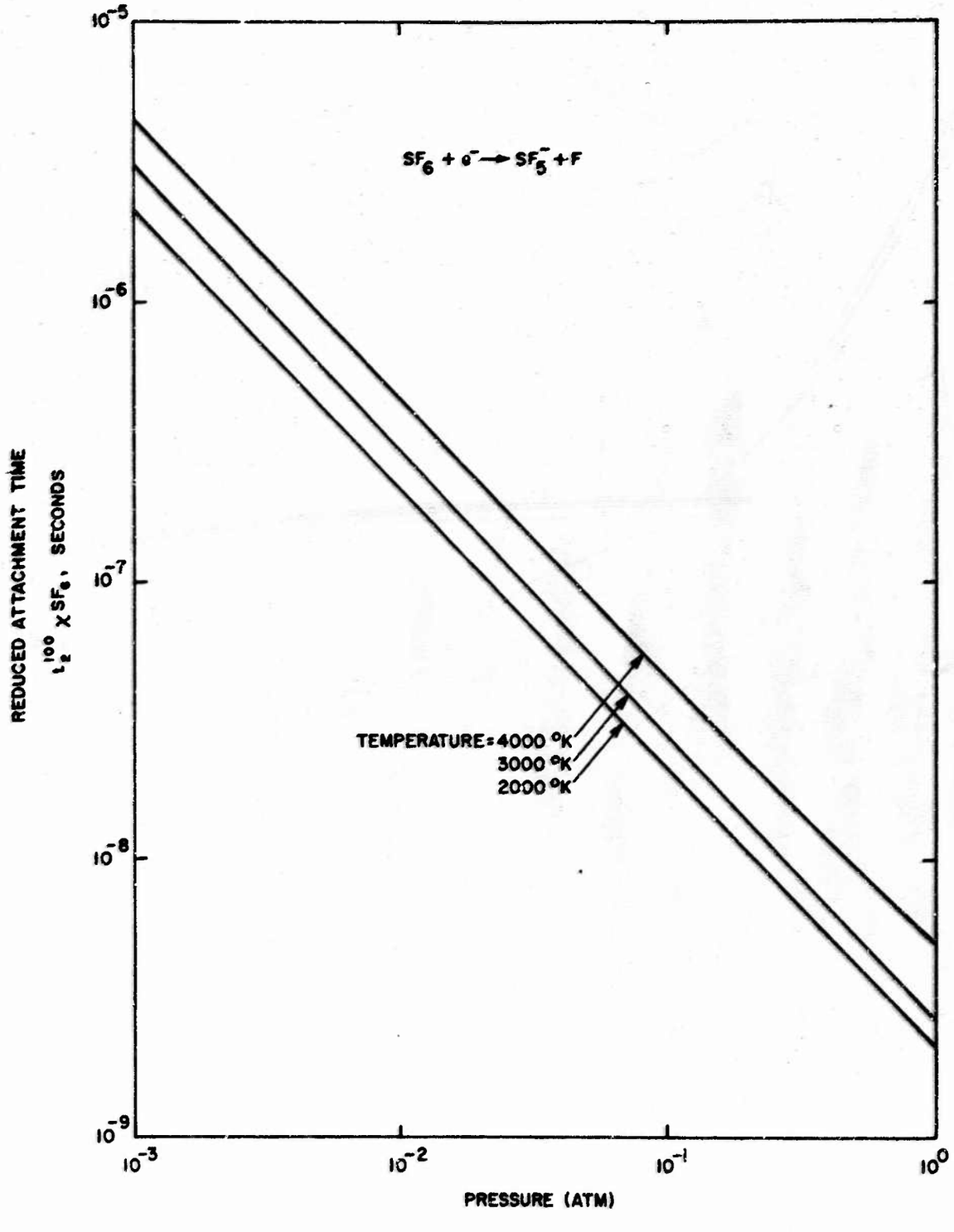

Figure 21. Dissociative Electron Attachment Time

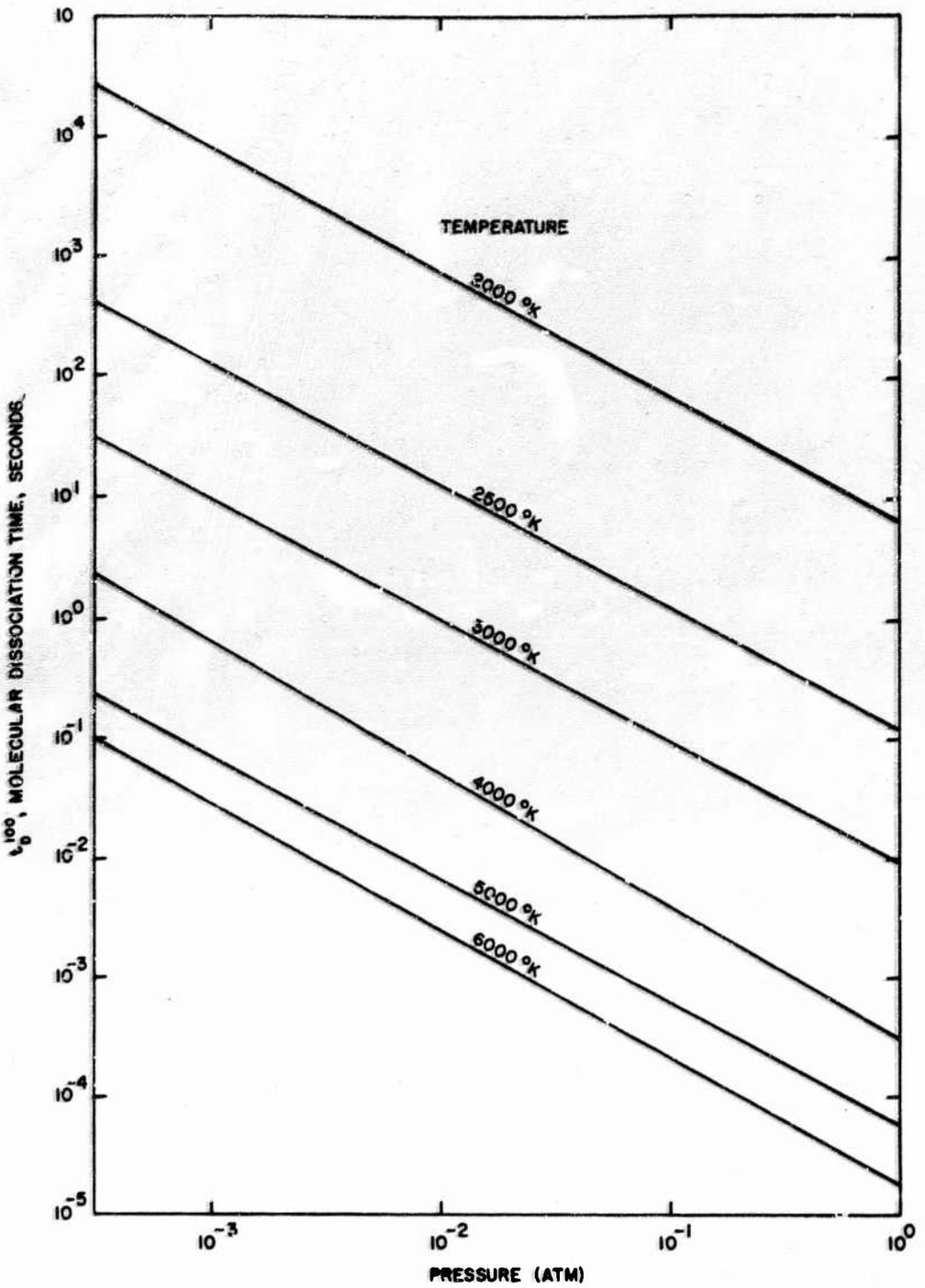

Figure 22. Molecular Dissociation Time

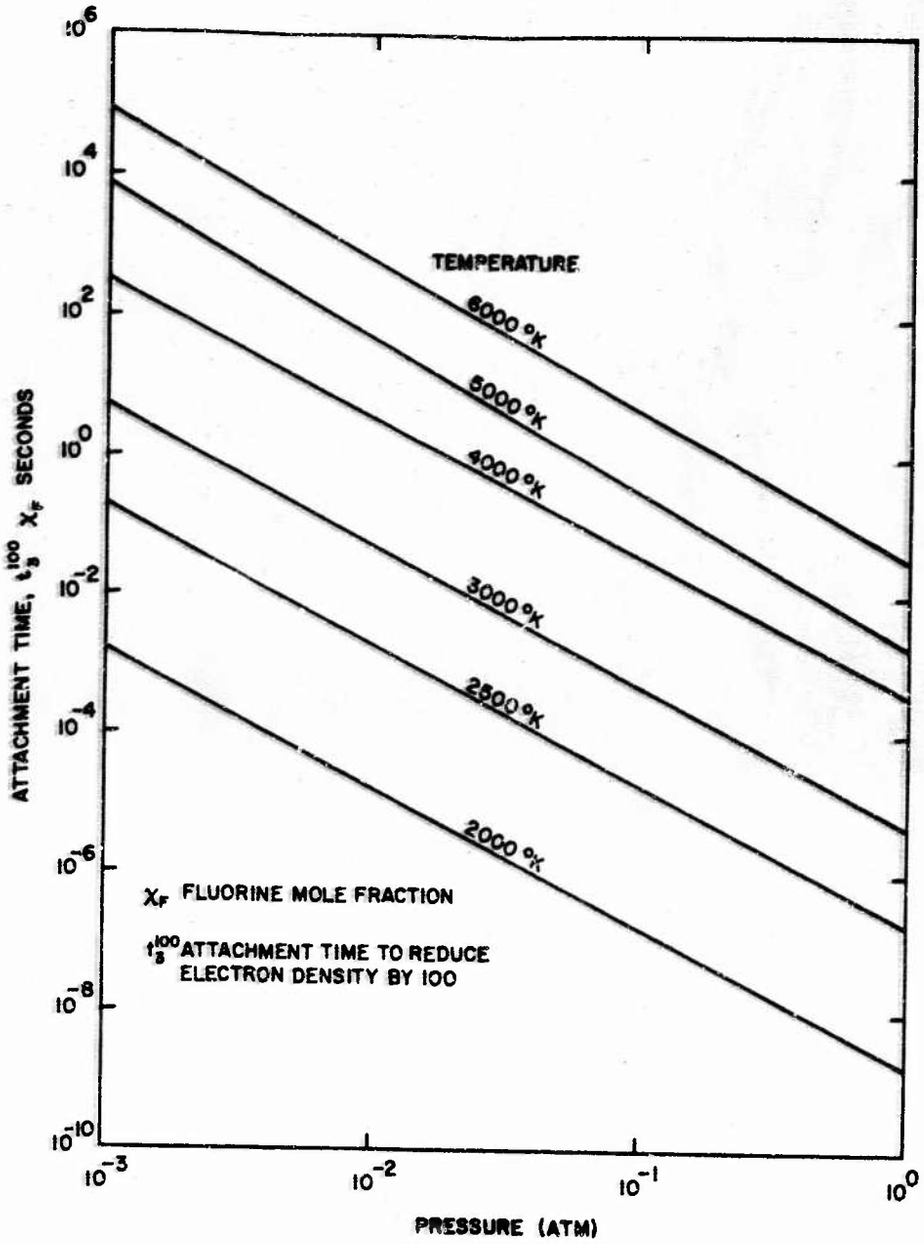

Figure 23. Electron Attachment Time

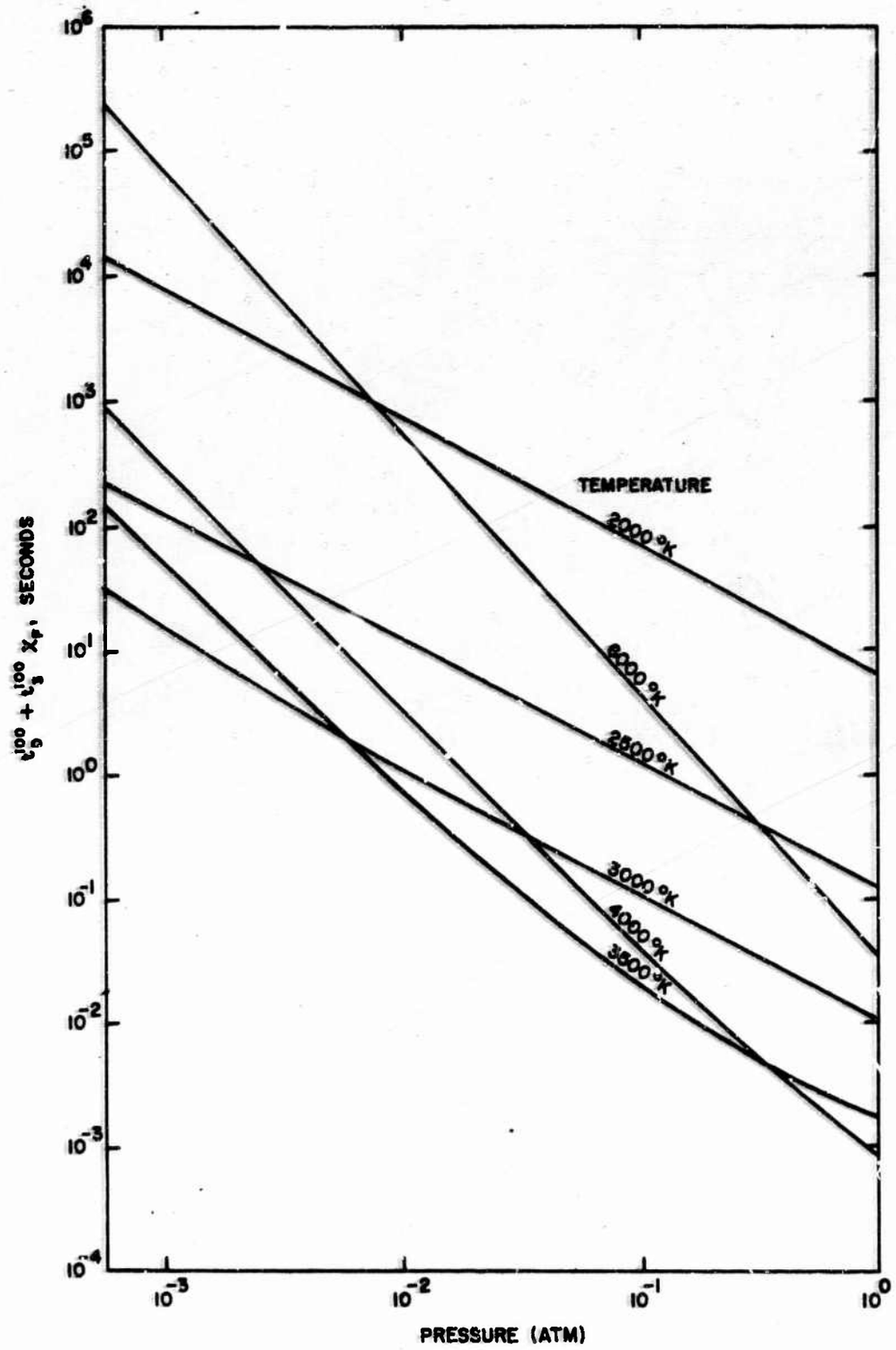

Figure 24. Total Time to Form Atomic Fluorine and Attach Electrons

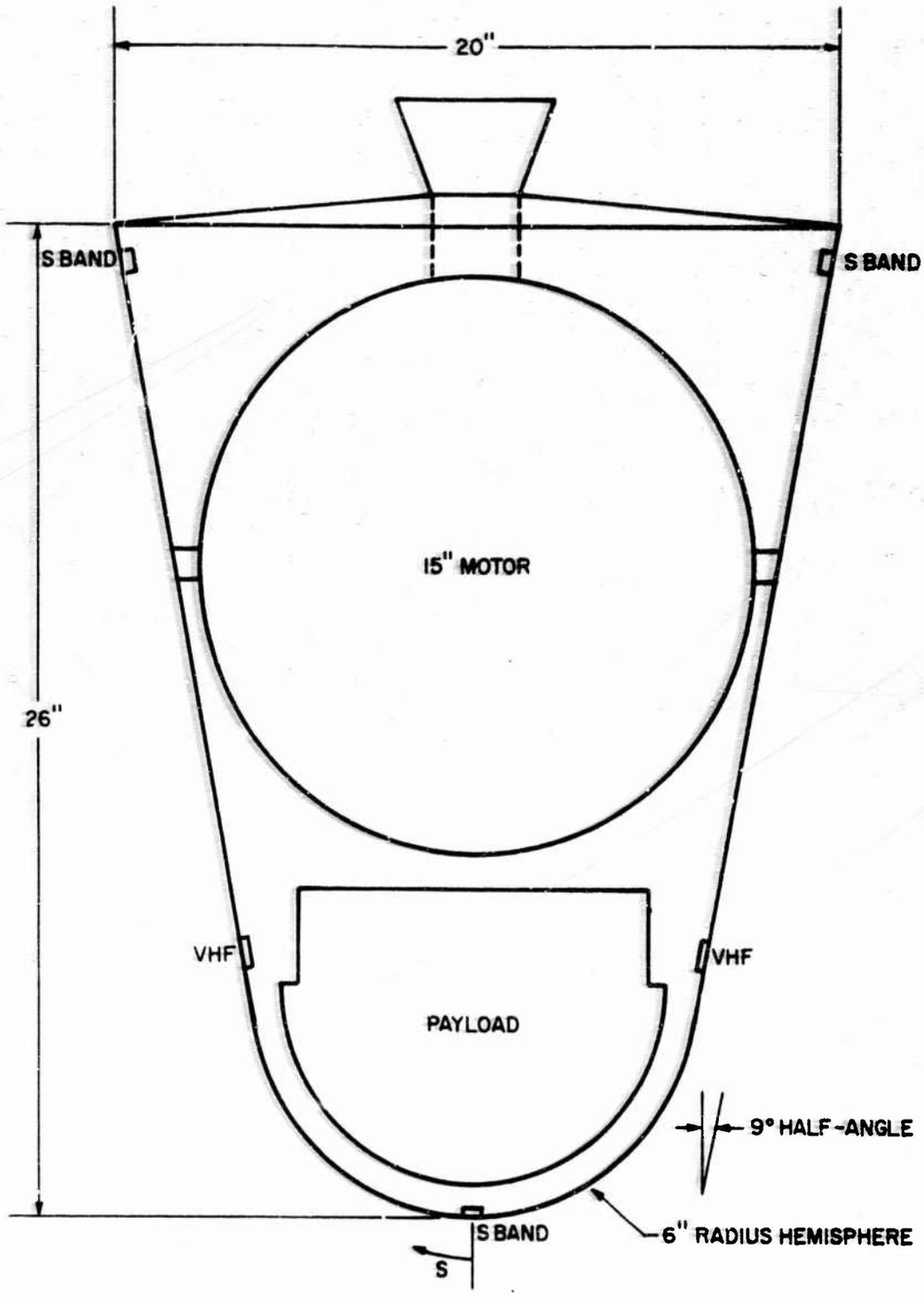

Figure 25. Trailblazer II Vehicle

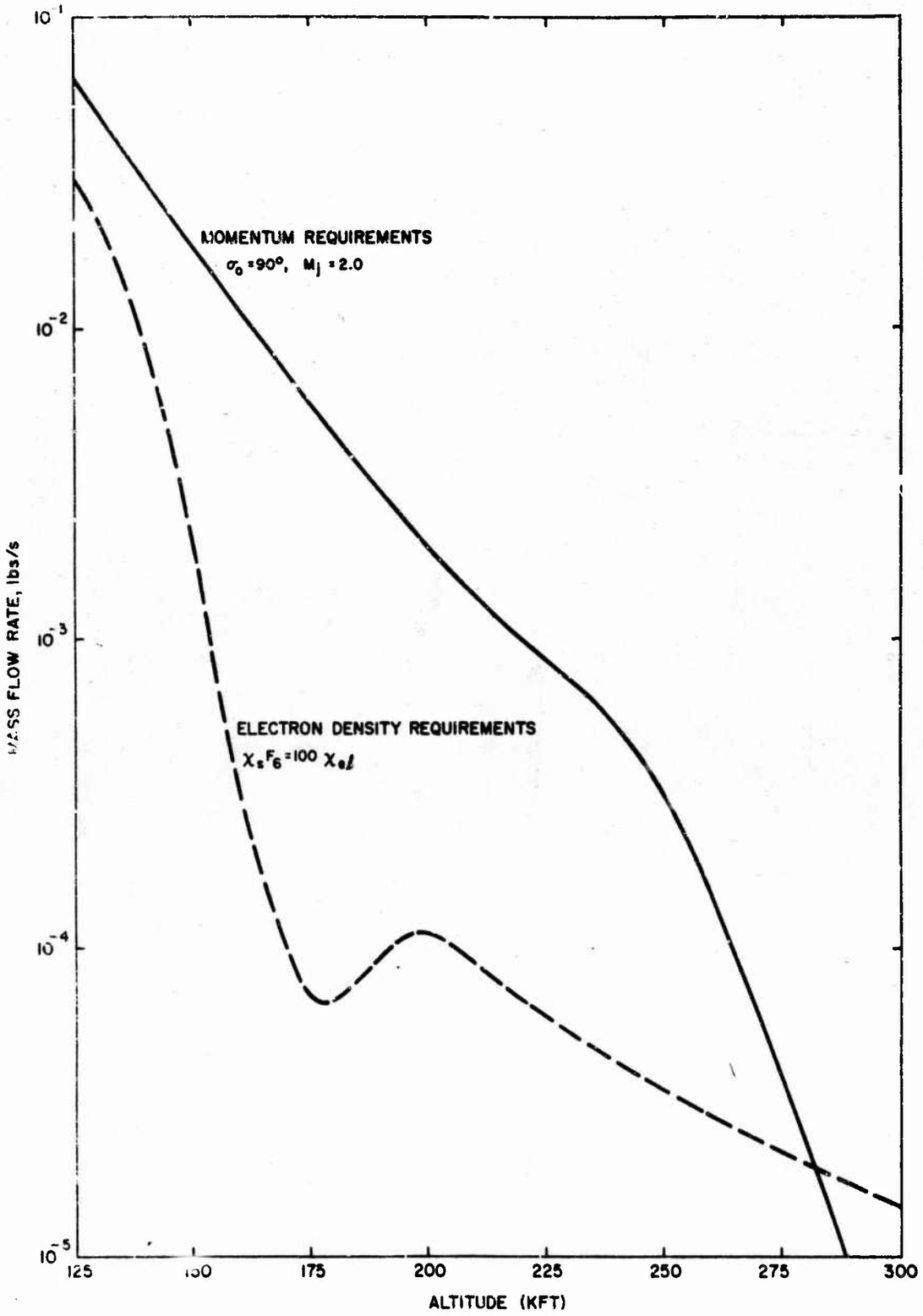

Figure 26. Mass Flow Requirements for Trailblazer II Re-entry

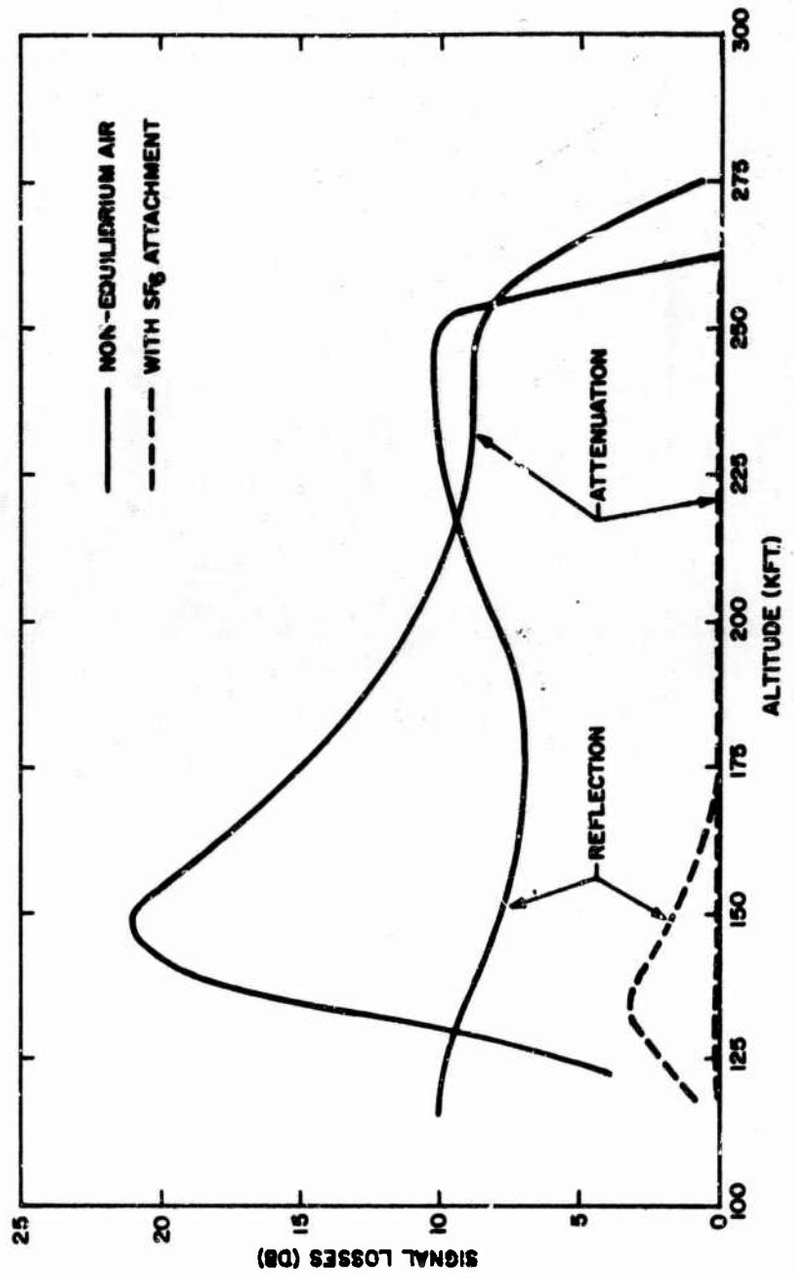

Figure 27. S-Band Transmission Losses

APPENDIX A

The derivatives dh_a/dx, du_a/dx, du_e/dx to be derived will be exact for a perfect gas since they were derived with this assumption; however, the form of the derivatives will be changed so that they can be used regardless of the thermodynamic state of the hot gas to be cooled. To form dh_a/dx, the derivative is

$$\frac{dh_a}{dx} = C_{P_a} \cdot \frac{dT_a}{dx} \tag{A1}$$

Differentiating Equation 3.7 gives

$$\frac{dh_a}{dx} = -2\lambda C_{P_a}\left(T_{a_1} - T_f\right)e^{-2\lambda x} \tag{A2}$$

This derivative must now be put in a form which is a function of the temperature difference of the air and coolant streamtube. In this way, the derivative will have been defined with the assumption of a perfect gas and will still be applicable to any thermodynamic state as long as the function $(T_a - T_e)$ is being continuously determined. To eliminate $(T_{a_1} - T_f)$ from Equation A2, the perfect gas energy evaluatior of Equation 3.1 is used. First, this equation is rearranged to get,

$$\left(C_{P_a} + C_{Q_1} C_{P_c}\right)T_f = C_{P_a} T_{a_1} + C_{Q_1} C_{P_c} T_{c_1} + \frac{u_1^2}{2} \frac{C_{Q_1}}{1 + C_{Q_1}} \tag{A3}$$

Multiplying this equation by -1.0 and adding $(C_{P_a} + C_{Q_1} C_{P_c}) T_{a_1}$ to both sides, it can be solved for $(T_{a_1} - T_f)$, and the following equation can be obtained:

$$\left(T_{a_1} - T_f\right) = \frac{C_{Q_1} C_{P_c}\left(T_{a_1} - T_{c_1}\right) - \frac{u_1^2}{2} \frac{C_{Q_1}}{1 + C_{Q_1}}}{C_{P_a} + C_{Q_1} C_{P_c}} \tag{A4}$$

Substitution of Equation A4 into Equation A2 gives:

$$\frac{dh_a}{dx} = -2\lambda C_{P_a} e^{-2\lambda x} \left\{ \frac{C_{Q_1} C_{P_c}\left(T_{a_1} - T_{c_1}\right) - \frac{u_1^2}{2} \frac{C_{Q_1}}{1 + C_{Q_i}}}{1 + C_{Q_1} \frac{C_{P_c}}{C_{P_a}}} \right\} \tag{A5}$$

which is still not in the form desired, but by substituting for $e^{-2\lambda x}$ its equivalent as a function of $(T_a - T_c)$ the final form of dh_a/dx will be determined. If Equation 3.7 is subtracted from 3.8

$$(T_a - T_c) = \left(T_{a_1} - T_{c_1}\right) e^{-2\lambda x} \tag{A6}$$

Substituting the value of $e^{-2\lambda x}$ from the above equation into Equation A5 gives, after rearrangement, the final form of dh_a/dx.

$$\frac{dh_a}{dx} = -\frac{2\lambda C_{Q_1}}{1 + C_{Q_1} \frac{C_{P_c}}{C_{P_a}}} \left\{ C_{P_c} - \frac{u_1^2}{2\left(1 + C_{Q_1}\right)\left(T_{a_1} - T_{c_1}\right)} \right\} (T_a - T_c) \tag{A7}$$

The derivatives of air and coolant streamtube velocity with streamtube distance can be found in analogous fashion by differentiating Equations 3.4 and 3.5 directly to get

$$\frac{du_a}{dx} = -\lambda\left(u_{a_1} - u_f\right)e^{-\lambda x} \tag{A8}$$

$$\frac{du_c}{dx} = \lambda u_f\, e^{-\lambda x} \tag{A9}$$

Now u_f must be eliminated and a value which is a function of the air and coolant streamtube velocity difference must be substituted for $e^{-\lambda x}$. The final velocity is known from Equation 3.6, and a relation for $e^{-\lambda x}$ can be derived by subtracting Equation 3.5 from Equation 3.4. This gives

$$\frac{u_a - u_c}{u_{a_1}} = e^{-\lambda x} \tag{A10}$$

Substituting this and the expression for u_f from Equation 3.6 into Equations A8 and A9 gives the final form of the velocity derivatives as,

$$\frac{du_a}{dx} = -\lambda\left(\frac{C_{Q_1}}{1 + C_{Q_1}}\right)(u_a - u_c) \tag{A11}$$

$$\frac{du_c}{dx} = +\lambda\left(\frac{1}{1 + C_{Q_1}}\right)(u_a - u_c) \tag{A12}$$

APPENDIX B

1. Outline of Non-Equilibrium Cooling Computer Program

To analyze the cooling of a chemically reacting airstream, assume that all chemical reactions occur in a streamtube adjacent to a streamtube composed only of SF_6 which remains a non-reacting gas. Cooling occurs due to the energy and momentum exchange between these two streamtubes.

2. Reacting Streamtube

The formulation for the analysis of the reacting streamtube is taken from Reference 5. In general, the non-equilibrium state of a gas is defined by two state variables such as pressure, P, and density, ρ, plus the additional variables $q_1, q_2, \ldots, q_n$ necessary to specify the internal non-equilibrium of the gas. The enthalpy then is given by an equation of state of the form:

$$h = h(P, \rho, q_1, \ldots, q_n) \tag{B1}$$

and the variables q_n are defined by a rate equation of the general form

$$\frac{Dq_k}{Dx} = \omega_k (P, \rho, q_1, \ldots, q_n) \tag{B2}$$

where Dq_k/Dx is the substantial derivative, and the ω_k are in general complicated functions of the thermochemical state. If the rotation of polyatomic molecules is completely excited at its equilibrium value and the effects of electronic excitation and ionization are negligible, the specify internal energy per mole of a specie including the effects of

vibration and dissociation is

$$\hat{e}_i = \hat{C}_{v_i} T + \hat{e}_{v_i} - \hat{e}_{D_i} \qquad \text{(B3)}$$

where:

$\hat{C}_{v_i}$ = specific heat per mole at constant volume

$\hat{e}_{v_i}$ = specific vibrational energy of specie

$\hat{e}_{D_i}$ = specific dissociation energy

The total internal energy of specie, i, of the reacting gas mixture is found by summing over all the species to give

$$e = \sum n_i \left(\hat{C}_{v_i} T + \hat{e}_{v_i} - \hat{e}_{D_i} \right) , \ \frac{\text{energy}}{\text{gm}} \qquad \text{(B4)}$$

The temperature T is related to the previous state variable by an equation of state

$$P = \rho \sum_i n_i \hat{R} T \qquad \text{(B5)}$$

Equation B5 is the same as the familiar state equation for an equilibrium gas (air)

$$P = \rho \left(\frac{\hat{R}}{\mu_o} \right) T Z \qquad \text{(B6)}$$

with

$$\sum n_i = z/\mu_o$$

$$\mu_o =$$

By using the definition of enthalpy as

$$h \equiv e + P/\rho \tag{B7}$$

Equations B4 and B5 can be used with

$$\hat{C}_{P_i} = \hat{C}_{v_i} + \hat{R}$$

to determine:

$$h = \frac{P}{\rho} \frac{\sum n_i \left(\hat{C}_{P_i}/\hat{R}\right)}{\sum n_i} + \sum n_i \left(\hat{e}_{v_i} - \hat{e}_{D_i}\right) \tag{B8}$$

which is a special form of the state relation $h=h(P, \rho, q_1, \ldots, q_n)$ applicable to a mixture of reacting gases. The rate equation (Equation B2) must now be generalized into a form applicable for the determination of the species n_i.

The present computer program considers seven chemical species O_2, N_2, NO, NO^+, e^-, O, N. The system of ten reactions are represented as

$$\sum \alpha_{r,i}\, x_i \underset{k_{b_r}}{\overset{k_{f_r}}{\rightleftharpoons}} \sum \beta_{r,i}\, x_i \tag{B9}$$

where x_i denote the chemical species listed in order above and $\alpha_{r,i}$ and $\beta_{r,i}$ are the stoichiometric coefficients of the reactants as given in Table B-I. All the reactions are listed in Table B-II. k_{f_r}, k_{b_r} are the forward and backward rate constants which are solely a function of temperature in the following way.

$$k_{f_r} = A''(T)^{c''} \exp \frac{D''}{T} \tag{B10a}$$

$$k_{b_r} = A'(T)^{c'} \exp \frac{D'}{T} \tag{B10b}$$

The coefficients of the above two equations have been taken from Reference 5 and are tabulated in Table B-III. With this notation the rate of change of the densities for the chemical species becomes

$$\left.\frac{dn_i}{dx}\right|_{\text{dissociation}} = \frac{1}{\rho u} \sum_{r=1}^{10} (\beta_{r,i} - \alpha_{r,i})\, k_{f_r} \prod_i (\rho n_i)^{\alpha_{r,i}} \tag{B11a}$$

$$\left.\frac{dn_i}{dx}\right|_{\text{recombination}} = \frac{1}{\rho u} \sum_{r=1}^{10} (\beta_{r,i} - \alpha_{r,i})\, k_{b_r} \prod_i (\rho n_i)^{\beta_{r,i}} \tag{B11b}$$

and the net rate of change of species is then

$$\frac{dn_i}{dx} = \left(\frac{dn_i}{dx}\right)_{\text{diss.}} - \left(\frac{dn_i}{dx}\right)_{\text{recom.}} \tag{B12}$$

The vibrational energy of the molecules is evaluated from the following expressions:

$$\frac{de_{v_i}}{dx} = \frac{e_{v_{i,eq}} - e_{v_i}}{u\tau_i} + \frac{e_{D_i} - e_{v_i}}{n_i} \left(\frac{dn_i}{dx}\right)_{recomb.}$$

$$- \left[\frac{\theta_{v_i} \hat{R}}{e^{\theta_{v_i}/T_M} - 1} - \frac{N_{v_i} \theta_{v_i} \hat{R}}{e^{N\theta_{v_i}/T_M} - 1} - e_{v_i} \right] \frac{1}{n_i} \left(\frac{dn_i}{dx}\right)_{diss.} \qquad i=1,2 \qquad \text{(B13)}$$

where $e_{v_{i,eq}}$ and T_M, $\frac{1}{\tau_i}$ are defined as

$$e_{v_{i,eq}} = \frac{\hat{R}\ \theta_{v_i}}{\exp\left(\frac{\theta_{v_i}}{T}\right) - 1} \qquad i=1,2$$

$$\frac{1}{T_M} = \frac{1}{T_V} - \frac{1}{T}$$

$$\frac{1}{\tau_i} = g_i\, \xi_i\, P(x) \exp(h_i T^{1/3}) \qquad i=1,2$$

and T_V, the vibrational temperature of the species, is defined as

$$T_{v_i} = \frac{\theta_{v_i}}{\ell n\left[\frac{\hat{R}\,\theta_{v_i}}{e_{v_i}} + 1\right]} \qquad \text{(B14)}$$

The constants θ_{v_i}, N_{v_i}, N, g_i, ξ_i, h_i for each specie are shown in Table B-IV.

3. Computer Program Inputs and Computation Procedure

Inputs to the non-equilibrium flow cooling program are:

1. initial properties of air and coolant

   T_{c_1}, T_{a_1}, u_{a_1}, C_{P_c}, P_{TOT}

2. cooling rate, and amount of coolant

   λ, G_Q

3. point at which cooling inititates

   x_c

4. integration step size

   Δx

The initial composition of the air streamtube, the total enthalpy of both the air and coolant streamtubes, and the above derivatives can be computed with these inputs. These derivatives, together with the derivatives for dn_i/dx and de_{v_i}/dx, allow the computation to proceed downstream in the following way:

$$h_a(x_{i+1}) = h_a(x_i) + \frac{dh_a}{dx}(x_i)\,\Delta x \qquad \text{(B15a)}$$

$$u_a(x_{i+1}) = u_a(x_i) + \frac{du_a}{dx}(x_i)\,\Delta x \qquad \text{(B15b)}$$

$$u_c(x_{i+1}) = u_c(x_i) + \frac{du_c}{dx}(x_i)\,\Delta x_i \qquad \text{(B15c)}$$

$$e_{v_i}(x_{i+1}) = e_{v_i}(x_i) + \frac{de_{v_i}}{dx}(x_i)\,\Delta x_i \qquad \text{(B15d)}$$

$$n_i(x_{i+1}) = n_i(x_i) + \frac{dn_i}{dx}(x_i)\,\Delta x \qquad \text{(B15e)}$$

Knowing $h_a(x)$ and $n_a(x)$ a new stagnation enthalpy of the air streamtube can be evaluated as follows:

$$H_a(x_{i+1}) = \frac{u_a^2}{2}(x_{i+1}) + h_a(x_{i+1}) \qquad \text{(B16)}$$

This also forms the stagnation enthalpy of the coclant from Equation 3.1

$$H_c(x_{i+1}) = \frac{\overline{HH} - H_a(x_{i+1})}{C_Q} \qquad \text{(B17)}$$

where

$$\overline{HH} = (H_a + C_Q H_c)_{\text{initial}}$$

Since the velocity of the coolant streamtube has been calculated, the definition of stagnation enthalpy can be used to find the static enthalpy of the coolant;

$$h_c(x_{i+1}) = H_c(x_{i+1}) - \frac{u_c^2}{2}(x_{i+1}) \qquad \text{(B18)}$$

Also, since the coolant is assumed to be undissociated and to remain a perfect gas, the temperature of the coolant is immediately found as follows:

$$T_c(x_{i+1}) = h_c(x_{i+1})/C_{P_c} \qquad \text{(B19)}$$

The mixing which occurs when a coolant is injected into a hot air-stream has been postulated to take place at constant pressure. This condition is, of course, true at the initial and final states of the gases. However, during the mixing process itself, the temperature of the coolant and air streamtube are unequal and Dalton's law of partial pressures does not apply. Since the actual mixing process is a highly complicated one, the exact thermodynamic state of the air streamtube is not known and Dalton's law can be postulated to hold as an expedient that will allow the determination of air thermodynamic properties in this region, knowing that the correct final state will be reached with this assumption. Thus, assume that

$$P_{TOT} = P_{air} + P_{coolant}$$

$$= \rho_a \Sigma n_i \hat{R} T_a + \rho_c \frac{\hat{R}}{m_c} T_c \qquad \text{(B20)}$$

where

a = air streamtube

c = coolant streamtube

n_i = number of moles per gram of species in air streamtube

$\hat{R}$ = universal gas constant

m = molecular weight

The air and coolant streamtube densities at any point in time is from Reference 1, as follows:

$$\rho_c = \left(\frac{C}{1-C}\right) \rho_a \qquad \text{(B21)}$$

Upon substitution of the above, Equation B-20 becomes

$$\rho_a \left[\sum_i n_i \hat{R}\, T_a + \frac{C}{1-C} \cdot \frac{\hat{R}}{m_c}\, T_c \right] = P_{TOT} \qquad \text{(B22)}$$

From Equations B5 and B8, $\Sigma n_i \hat{R}\, T_a$ can be solved in terms of an energy (enthalpy) relation and substituting in the above equation gives

$$\rho_a \left[\left\{ h_a(x) - \sum_i n_i \left(e_{v_i} - e_{D_i} \right) \right\} \frac{\sum_i n_i}{\sum_i n_i \left(\frac{\hat{C}_{P_i}}{\hat{R}} \right)} + \frac{C}{1-C} \cdot \frac{\hat{R}}{m_c}\, T_c \right] = P_{TOT} \qquad \text{(B23)}$$

Assume now that mixing proceeds at the same rate as the momentum exchange,

$$C = \frac{u_{a_1} - u_a}{u_a}$$

At the initial point with no coolant injected into the air streamtube $u_a = u_{a_1}$, and $C_{initial} = 0$, and the final value of C with $u_a = u_f$ gives

$$C_f = \frac{C_Q}{1 + C_Q}$$

Having specified C in terms of the velocity slowdown of the air streamtube, $\frac{u_{a_1}}{u_a} - 1$ can be substituted for C/1-C in Equation B23, and solving for the

air streamtube density

$$\rho_a = \frac{P_{TOT}}{\left[\left\{h_a(x) - \sum_i n_i\left(e_{v_i} - e_{D_i}\right)\right\} \frac{\Sigma n_i}{\Sigma n_i \frac{\hat{C}_{P_i}}{\hat{R}}} + \left(\frac{u_{a_1}}{u_a} - 1\right) \frac{\hat{R}}{m_c} T_c\right]} \tag{B24}$$

Once the density and the bracketed terms are found, the air streamtube temperature can be determined by using the partial pressure relation Equation B-20 to get

$$T_A = \frac{P_a}{\rho_a \sum_i n_i \hat{R}} \tag{B25}$$

and knowing T_a, T_c, u_a, u_c new derivatives can be formed for

$$\frac{dh_a}{dx}, \frac{du_a}{dx}, \frac{du_c}{dx}, \frac{dn_i}{dx}, \frac{de_{v_i}}{dx}$$

and the computation process can be continued until $T_a = T_c$ and $u_a = u_c$ at which point the reacting air streamtube and the coolant streamtube will have exchanged all the energy available and computation stops. A typical output of the program is shown on the pages along with a listing of the computer program instructions.

Non-Equilibrium Cooling Computer Program Listing

MAIN--

```
C       MAIN PROGRAM FOR FLOW OF A NITROGEN OXYGEN MIXTURE
        COMMON FMTA,FMTB,FMTC,IDENT,LINE,X,H,RO,T,P,U,A,TV,DNDXD,DNDX,DENS
       1,ROFREE,PFREE,IM,SMALLR,PO,XO
        DIMENSION FMTA(96),FMTB(24),FMTC(12),FMTD(1),THETAV(2),VNV(2)
        DIMENSION AB(20),CB(20),DB(20),AF(20),CF(20),DF(20),CP(20),ED(20)
        DIMENSION ICB(20),ICF(20),IA(21,20),IB(21,20),BMA(20,20),IDENT(12)
        DIMENSION DENS(20),EV(20),V(2),TV(2),TAU(2),EVQ(2),EXC(2),EXD(2)
        DIMENSION RKB(20),RKF(20),DNDXD(20),DNDXR(20),DNDX(20),DEVDX(2)
        EQUIVALENCE ((MAD,FIMAD),(IMAX,FIMAX)
C           SET UP CONSTANTS FOR CALCULATIONS
        R=8.31436E7
        THETAV(1)=2238.97
        THETAV(2)=3336.8
        VNV(1)=52.
        VNV(2)=67.
C           READ IN FORMAT STATEMENTS FOR OUTPUT
        READ INPUT TAPE 5,1001,(FMTA(J),J=1,96),(FMTB(J),J=1,24),(FMTC(J),
       1J=1,12)
C           READ IN DATA TO DEFINE REACTIONS
        READ INPUT TAPE 5,1002,IMAX,IRMAX,(AB(K),CB(K),DB(K),K=1,IRMAX),(A
       1F(K),CF(K),DF(K),K=1,IRMAX)
C           EVALUATE COEFFICIENTS FOR POWER OF T IN RATE CONSTANTS
        DO 3 K=1,IRMAX
        ICB(K)=2.0*CB(K)+SIGNF(0.5,CB(K))
        ICF(K)=2.0*CF(K)+SIGNF(0.5,CF(K))
 3      CONTINUE
        IFM=IMAX/10
        IF(IFM) 6,6,5
C           SET UP FORMAT TO READ IN A AND B COEFFICIENTS
 5      IMAD=IMAX+54*IFM
        GO TO 7
B6      FIMAD=FIMAX+006000000000
B7      FMTD=FIMAD+740000310134
        READ INPUT TAPE 5,FMTD,(((IA(J,K),J=1,IMAX),K=1,IRMAX),(((IB(J,K),J=
       11,IMAX),K=1,IRMAX)
        READ INPUT TAPE 5,1003,(CP(J),J=1,IMAX)
        READ INPUT TAPE 5,1004,(ED(J),J=1,IMAX)
C           EVALUATE COEFFICIENT FOR POWER OF MASS DENSITY IN RATE EQUATION
        DO 9 K=1,IRMAX
        IA(IMAX+1,K)=-1
        IB(IMAX+1,K)=-1
        DO 8 J=1,IMAX
C           CALCULATE  B - A
        BMA(J,K)=IB(J,K)-IA(J,K)
        IA(IMAX+1,K)=IA(IMAX+1,K)+IA(J,K)
        IB(IMAX+1,K)=IB(IMAX+1,K)+IB(J,K)
 8      CONTINUE
 9      CONTINUE
        DO 10 J=3,IMAX
        EV(J)=0.0
 10     CONTINUE
        IM=IMAX-1
C           READ IN JOB IDENTIFICATION AND INITIAL CONDITIONS
   12 READ INPUT TAPE 5,1005,(IDENT(J),J=1,12),X,T,U,P,XC,ALAMBA,CQ,TC,C
      1PC,ANC,HILLNO,(EV(J),J=1,2),(DENS(J),J=1,IM)
```

```
MAIN--

C         INITIALIZE PRINTED AND PUNCHED OUTPUT
      WRITE OUTPUT TAPE 6,1101,(IDENT(J),J=1,12)
      LINE=2
 1965 DENS(IMAX)=0.0
C         CALCULATE DENSITY FOR SUMMATION NI
      DO 14 J=1,IM
      DENS(IMAX)=DENS(IMAX)+DENS(J)
   14 CONTINUE
      RO=P/(T*R*DENS(IMAX))
      FLOW =RO*U
      DUMA=0.0
      DUMB=0.0
      CORR=-2.8935E11
C         CALCULATE THE STAGNATION ENTHALPY
      DO 17 J=1,IM
      DUMA=DUMA+DENS(J)*CP(J)
      DUMB=DUMB+DENS(J)*(EV(J)-ED(J))
   17 CONTINUE
      DO 19 J=1,2
      TV(J)=THETAV(J)/LOGF(R*THETAV(J)/EV(J)+1.0)
   19 CONTINUE
      HT=P*DUMA/(RO*DENS(IMAX))+DUMB+0.5*U*U
      H=HT-0.5*U*U
      UAZERO=U
   80 AHA=1.+CQ
      CPCOOL=CPC*R*ANC
      COOL=CPCOOL*CQ
      UPRIME =0.
      NUMBER=0
C         READ IN AN INCREMENT CARD
   26 READ INPUT TAPE 5,1006,NSI,IFNI,NI,DELX
      IF(NSI) 12,12,1963
 1963 WRITE OUTPUT TAPE 6,1104,NSI,IFNI,NI,DELX
      LINE =LINE+2
      IFHEAD=1000*IFNI+NSI-NI
      IF (IFHEAD) 29,27,27
C         PRINT HEADINGS IF THERE WILL BE OUTPUT FOR THIS INCREMENT CARD
   27 WRITE OUTPUT TAPE 6,FMTA
      LINE=LINE+7
      IF(IFNI) 29,29,28
   28 CALL OUT
C         SUBDIVIDE CALCULATION IF MORE THAN 150 STEPS
   29 NLIM=1500-XMODF(1500,NI)
      IF(NSI-NLIM) 30,30,31
   30 NLIM=NSI
   31 NSI=NSI-NLIM
      NCOUNT=NI
C         CALCULATE DERIVATIVES AND NEW VALUES FOR ALL VARIABLES
      DO 100 N=1,NLIM
      TCURT=T**0.33333333
      TAU(1)=4.924E-5*P*EXPF(0.6464*TCURT)
      TAU(2)=1.28E-5*P*EXPF(0.5493*TCURT)
      V(1)=1.0
      V(2)=1.0
      TSQ=SQRTF(T)
      DO 45 K=1,IRMAX
```

```
MAIN--

      RKB(K)=AB(K)*POWER(ICB(K),TSQ)*EXPF(CB(K)/T)
      RKF(K)=AF(K)*POWER(ICF(K),TSQ)*EXPF(DF(K)/T)
      DO 43 J=1,2
      RKF(K)=RKF(K)*POWER(IA(J,K),V(J))
43    CONTINUE
45    CONTINUE
      DO 55 I=1,IM
      DD=0.0
      DR=0.0
      DO 54 K=1,IRMAX
      IF(BMA(I,K)) 47,54,47
47    DUMD=BMA(I,K)*RKF(K)
      DUMR=BMA(I,K)*RKB(K)
      DO 51 J=1,IMAX
      DUMD=DUMD*POWER(IA(J,K),DENS(J))
      DUMR=DUMR*POWER(IB(J,K),DENS(J))
51    CONTINUE
      LA=IA(IMAX+1,K)
      LB=IB(IMAX+1,K)
      DD=DD+DUMD*POWER(LA,RO)
      DR=DR+DUMR*POWER(LB,RO)
54    CONTINUE
      DNDXD(I)=DD/U
      DNDXR(I)=DR/U
      DNDX(I)=DNDXD(I)-DNDXR(I)
55    CONTINUE
      DO 63 J=1,2
 201  EXA=EXPF(THETAV(J)/T)
      EVQ(J)=R*THETAV(J)/(EXA-1.0)
      DEVDX(J)=(EVQ(J)-EV(J))*TAU(J)/U
      EV(J)=EV(J)+DEVDX(J)*DELX
      TV(J)=THETAV(J)/LOGF(R*THETAV(J)/EV(J)+1.0)
63    CONTINUE
      DENS(IMAX)=0.0
      DUMA=0.0
      DUMB=0.0
      DO 65 J=1,IM
      DENS(J)=DENS(J)+DNDX(J)*DELX
      DENS(IMAX)=DENS(IMAX)+DENS(J)
      DUMA=DUMA+DENS(J)*CP(J)
      DUMB=DUMB+DENS(J)*(EV(J)-ED(J))
65    CONTINUE
      X=X+DELX
      IF(X-XC) 79,83,83
  83  IF (NUMBER-1) 82,81,81
  82  HH=HT+COOL*TC
      NUMBER=NUMBER+1
  81  BAH=(U-UPRIME)/AHA
      UPDX=ALAMBA*BAH
      UPRIME=UPRIME+UPDX*DELX
      DUDX=-UPDX*CQ
      U=U+DUDX*DELX
      HT=H+.5*U*U
      HTPRIM=HH-HT
      HPRIME=(HTPRIM/CQ)-0.5*UPRIME*UPRIME
      TPRIME=HPRIME/CPCOOL
```

Non-Equilibrium Cooling Computer Program Listing (Concluded)

```
MAIN--

      DHDX=-CQ/(1.+CQ*HILLNO)*(CPCOOL-U*U/(2.0*AHA*(T-TC)))*ALAMBA*(T-TP
     1RIME)
      H=H+DHDX*DELX
   79 OUTH=(H-CORR)/7.874E8
      RC=P/((H-DUMB)*DENS(IMAX)/DUMA+(UAZERO/U-1.0)*ANC*R*TPRIME)
      PA=P-(UAZERO/U-1.0)*RO*R*ANC*TPRIME
      T=PA/(RO*R*DENS(IMAX))
      A=FLOW/(RO*U)
      NCOUNT=NCOUNT-1
C        PRINT OUT VARIABLES IF REQUIRED
      IF(NCOUNT) 71,71,100
 71   CALL OUT
      NCOUNT=NI
 100  CONTINUE
      IF(IFNI*(NI-NCOUNT)) 105,110,105
 105  CALL OUT
 110  IF(IFHEAD) 120,115,115
C        IF THERE HAS BEEN OUTPUT FOR THIS INCREMENT CARD PRINT OUT
C        VALUES OF VARIABLES FOR RESTART OF CALCULATIONS AND INITIALIZE
C        PRINTED OUTPUT
  115 WRITE OUTPUT TAPE 6,1102,(EV(J),J=1,2),FLOW,OUTH,TPRIME,UPRIME,HPR
     1IME
      WRITE OUTPUT TAPE 6,1101,(IDENT(J),J=1,12)
      LINE=2
 120  IF(NSI) 29,26,29
 1001 FORMAT(12A6)
 1002 FORMAT(2I5/(E20.5,F10.1,F20.0))
 1003 FORMAT(10F7.2)
 1004 FORMAT(6E12.3)
 1005 FORMAT(12A6/4E15.5/3E15.5/4E15.5/2E15.5/(4E15.5))
 1006 FORMAT(3I5,1PE15.5)
 1101 FORMAT(43H1NITROGEN-OXYGEN FLOW THROUGH A STREAM TUBE/1X,12A6)
 1102 FORMAT(27HOVIBRATIONAL ENERGY OF O2 =,1PE15.7/27H VIBRATIONAL ENER
     1GY OF N2 =,1PE15.7/17H MASS FLOW RATE =,1PE15.7/11H ENTHALPY =,1PE
     215.5/9HOTPRIME =,1PE15.5/9H UPRIME =,1PE15.5/9H HPRIME =,1PE15.5)
 1103 FORMAT(11A6,6X,A6,1HO,I1)
 1104 FORMAT(15HOINCREMENT CARD,3I5,1PE10.2)
      END(1,1,0,0,0,1,1,1,0,0,0,0,0,0,0)
```

TABLE B-I

STOICHIOMETRIC COEFFICIENTS

$d_{r,i}$

r \ i	O_2	N_2	NO	NO^+	e^-	O	N	M
1	2	0	0	0	0	0	0	0
2	1	0	0	0	0	1	0	0
3	1	0	0	0	0	0	0	1
4	0	2	0	0	0	0	0	0
5	0	1	0	0	0	0	0	1
6	0	0	1	0	0	0	0	1
7	1	0	0	0	0	0	1	0
8	0	1	0	0	0	1	0	0
9	1	1	0	0	0	0	0	0
10	0	0	0	0	0	1	1	0

$B_{r,i}$

r \ i	O_2	N_2	NO	NO^+	e^-	O	N	M
1	1	0	0	0	0	2	0	0
2	0	0	0	0	0	3	0	0
3	0	0	0	0	0	2	0	1
4	0	1	0	0	0	0	2	0
5	0	0	0	0	0	0	2	1
6	0	0	0	0	0	1	1	1
7	0	0	1	0	0	1	0	0
8	0	0	1	0	0	0	1	0
9	0	0	2	0	0	0	0	0
10	0	0	0	1	1	0	0	0

$$M = \sum_i n_i$$

REACTIONS

TABLE B-II

$$\frac{dO_2}{dx} = \frac{1}{\rho u}\left[-k_{f_1}(\rho O)^2+k_{b_1}(\rho O)^2(\rho O_2)-k_{f_2}(\rho O_2)(\rho O)+k_{b_2}(\rho O)^3-k_{f_3}(\rho O_2)(\rho M)\right.$$
$$\left.+k_{b_3}(\rho O)^2(\rho M)-k_{f_7}(\rho O_2)(\rho N)+k_{b_7}(\rho NO)(\rho O)-k_{f_9}(\rho N_2)(\rho O_2)+k_{b_9}(\rho NO)^2\right]$$

$$\frac{dO}{dx} = \frac{1}{\rho u}\left[2k_{f_1}(\rho O_2)^2-2k_{b_1}(\rho O)^2(\rho O_2)+2k_{f_2}(\rho O_2)(\rho O)-2k_{b_2}(\rho O)^3+2k_{f_3}(\rho O_2)(\rho M)\right.$$
$$-2k_{b_3}(\rho O)^2(\rho M)+k_{f_6}(\rho NO)(\rho M)-k_{b_6}(\rho N)(\rho O)(\rho M)+k_{f_7}(\rho N)(\rho O_2)-k_{b_7}(\rho NO)(\rho O)$$
$$\left.-k_{f_8}(\rho O)(\rho N_2)+k_{b_8}(\rho NO)(\rho N)-k_{f_{10}}(\rho N)(\rho O)+k_{b_{10}}(\rho NO^+)(\rho e^-)\right]$$

$$\frac{dN_2}{dx} = \frac{1}{\rho u}\left[-k_{f_9}(\rho N_2)^2+k_{b_9}(\rho N_2)(\rho N)^2-k_{f_5}(\rho N_2)(\rho M)+k_{b_5}(\rho N)^2(\rho M)\right.$$
$$\left.-k_{f_9}(\rho N_2)(\rho O_2)+k_{b_9}(\rho NO)^2\right]$$

$$\frac{dN}{dx} = \frac{1}{\rho u}\left[+2k_{f_4}(\rho N_2)^2-2k_{b_4}(\rho N)^2(\rho N_2)+2k_{f_5}(\rho N_2)(\rho M)-2k_{b_5}(\rho N)^2(\rho M)\right.$$
$$+k_{f_6}(\rho NO)(\rho M)-k_{b_6}(\rho N)(\rho O)(\rho M)-k_{f_7}(\rho N)(\rho O_2)+k_{b_7}(\rho NO)(\rho O)$$
$$\left.+k_{f_8}(\rho O)(\rho N_2)-k_{b_8}(\rho NO)(\rho N)-k_{f_{10}}(\rho N)(\rho O)+k_{b_{10}}(\rho NO^+)(\rho e^-)\right]$$

$$\frac{dNO^+}{dx} = \frac{de^-}{dx} = \frac{1}{\rho u}\left[k_{f_{10}}(\rho N)(\rho O)-k_{b_{10}}(\rho NO^+)(\rho e^-)\right]$$

$$\frac{dNO}{dx} = \frac{1}{\rho u}\left[-k_{f_6}(\rho NO)(\rho M)+k_{b_6}(\rho N)(\rho O)(\rho M)+k_{f_7}(\rho N)(\rho O_2)-k_{b_7}(\rho NO)(\rho O)\right.$$
$$\left.+k_{f_8}(\rho O)(\rho N_2)-k_{b_8}(\rho NO)(\rho N)+2k_{f_9}(\rho N_2)(\rho O_2)-2k_{b_9}(\rho NO)^2\right]$$

TABLE B-III

REACTIONS AND RATE CONSTANTS

r	REACTION	A'	C'	D'	A''	C''	D''
1	$O_2 + O_2 \rightleftarrows 2O + O_2$	$3.0 \cdot 10^{18}$	-1.0	0	$3.6 \cdot 10^{21}$	-1.5	- 59,380.
2	$O_2 + O \rightleftarrows 2O + O$	$1.75 \cdot 10^{15}$	0	0	$2.1 \cdot 10^{18}$	- .5	- 59,380.
3	$O_2 + M \rightleftarrows 2O + M$	$1. \cdot 10^{18}$	-1.0	0	$1.2 \cdot 10^{21}$	-1.5	- 59,380.
4	$O_2 + N_2 \rightleftarrows 2N + N_2$	$1.6666 \cdot 10^{20}$	-1.5	-810.	$3. 10^{21}$	-1.5	-113,260.
5	$N_2 + M \rightleftarrows 2N + M$	$8.333 \cdot 10^{20}$	-1.5	-810.	$1.5 \cdot 10^{22}$	-1.5	-113,260.
6	$NO + M \rightleftarrows N+O+M$	$1.3 \cdot 10^{21}$	-1.5	-490.	$5.2 \cdot 10^{21}$	-1.5	- 75,490.
7	$N + O_2 \rightleftarrows NO + O$	$2.38 \cdot 10^{11}$	0.5	-19,136.	$1. 10^{12}$	0.5	- 3,120.
8	$O + N_2 \rightleftarrows NO + N$	$1.111 \cdot 10^{13}$	0	-500.	$5. 10^{13}$	0	- 38,000.
9	$N_2 + O_2 \rightleftarrows 2NO$	$4.814815 \cdot 10^{23}$	-2.5	-43,510.	$9.1 \cdot 10^{24}$	-2.5	- 65,000.
10	$N + O \rightleftarrows NO^+ + e^-$	$1.8 \cdot 10^{21}$	-1.5	0	$6.48 \cdot 10^{11}$	0	- 31,703.

$$k_{f_r} = A'' \, T^{C''} e^{D''/T}$$

$$k_{b_r} = A' \, T^{C'} e^{D'/T}$$

TABLE B-IV

MOLECULAR AND ATOMIC CONSTANTS

CONSTANT / i	O_2	N_2	NO	NO^+	e^-	O	N	M
$g_i \left(\frac{cm^2}{dyne - sec}\right)$	$4.924 \cdot 10^{-5}$	$1.28 \cdot 10^{-5}$	$2.092 \cdot 10^{-5}$	0	0	0	0	0
$h_i\ (^oK)^{-1/3}$	0.6464	0.5493	0.4198	0	0	0	0	0
$\theta_{v_i}\ (^oK)$	2238.97	3336.8	2699.18	3372.95	0	0	0	0
N_{v_i}	52	67	55	72	0	0	0	0
$C_{v_i}/\hat{R}$	5/2	5/2	5/2	5/2	0	3/2	3/2	0
$C_{P_i}/\hat{R}$	7/2	7/2	7/2	7/2	0	5/2	5/2	0
$e_{D_i}\left(\frac{exps}{mole}\right)$	$4.763 \cdot 10^{12}$	$9.185 \cdot 10^{12}$	$6.079 \cdot 10^{12}$	$1.02 \cdot 10^{13}$	0	0	0	0
$e_{I_i}\left(\frac{exps}{mole}\right)$	0	0	0	$8.93 \cdot 10^{12}$	0	0	0	0

$\hat{R} = 8.31436 \cdot 10^7$ exps/mole ^oK

$N_o = 6.0228 \cdot 10^{23}$ molecules/mole

UNCLASSIFIED

Security Classification

DOCUMENT CONTROL DATA - R&D

(Security classification of title, body of abstract and indexing annotation must be entered when the overall report is classified)

1. ORIGINATING ACTIVITY (Corporate author) MITHRAS, Inc. 701 Concord Ave Cambridge, Massachusetts 02138	2a. REPORT SECURITY CLASSIFICATION Unclassified 2b. GROUP

3. REPORT TITLE

AN INJECTION SYSTEM FOR ALLEVIATION OF RADIO BLACKOUT DURING RE-ENTRY

4. DESCRIPTIVE NOTES (Type of report and inclusive dates)

Scientific Report No. 2

5. AUTHOR(S) (Last name, first name, initial)

Good, R. Earl; Rossi, Joseph J.

6. REPORT DATE	7a. TOTAL NO. OF PAGES	7b. NO. OF REFS
January 1966	xii and 91	15

8a. CONTRACT OR GRANT NO.	9a. ORIGINATOR'S REPORT NUMBER(S)
AF 19(628)-3852 b. PROJECT NO 4642 c. Task No. 464202 d	MC 63-78-R2 9b. OTHER REPORT NO(S) (Any other numbers that may be assigned this report) AFCRL-66-160

10. AVAILABILITY/LIMITATION NOTICES

Distribution of this document is unlimited.

11. SUPPLEMENTARY NOTES	12. SPONSORING MILITARY ACTIVITY
N/A	Air Force Cambridge Research Labs Office of Aerospace Research USAF Bedford, Mass.

13. ABSTRACT

This report outlines method of creating a window for radio communication through a re-entry plasma sheath. The results of non-equilibrium numerical calculations illustrate that the injection of a coolant gas will reduce the plasma sheath temperature but will not reduce the free electron density or plasma frequency. Plasma electron density can be reduced, however, by attachment to electrophilic gases. The chemical rates of attachment are computed; and criteria are developed which specify the amount of electrophilic gas required to reduce the electron density a specified amount in a given time. As a practical application, a gas injection system for the total alleviation of S-band blackout throughout the re-entry of a Trailblazer II vehicle would have a total charged weight of 3.4 lbs., a volume of 215 in^3, and would discharge 0.28 lbs. of SF_6 during re-entry. With a pulsed injection system, an even smaller system can be used.

DD FORM 1 JAN 64 1473

UNCLASSIFIED

Security Classification

UNCLASSIFIED

Security Classification

14 KEY WORDS	LINK A		LINK B		LINK C	
	ROLE	WT	ROLE	WT	ROLE	WT
Re-entry communication		10				
Blackout		4				
Gas Injection		10				
Non-equilibrium cooling		2				
Trailblazer II		8				
Cross-jet flow		10				
Electrophilic gases		4				
SF_6		4				
Electron attachment		6				
De-ionization		10				

INSTRUCTIONS

1. ORIGINATING ACTIVITY: Enter the name and address of the contractor, subcontractor, grantee, Department of Defense activity or other organization *(corporate author)* issuing the report.

2a. REPORT SECURITY CLASSIFICATION: Enter the overall security classification of the report. Indicate whether "Restricted Data" is included. Marking is to be in accordance with appropriate security regulations.

2b. GROUP: Automatic downgrading is specified in DoD Directive 5200.10 and Armed Forces Industrial Manual. Enter the group number. Also, when applicable, show that optional markings have been used for Group 3 and Group 4 as authorized.

3. REPORT TITLE: Enter the complete report title in all capital letters. Titles in all cases should be unclassified. If a meaningful title cannot be selected without classification, show title classification in all capitals in parenthesis immediately following the title.

4. DESCRIPTIVE NOTES: If appropriate, enter the type of report, e.g., interim, progress, summary, annual, or final. Give the inclusive dates when a specific reporting period is covered.

5. AUTHOR(S): Enter the name(s) of author(s) as shown on or in the report. Enter last name, first name, middle initial. If military, show rank and branch of service. The name of the principal author is an absolute minimum requirement.

6. REPORT DATE: Enter the date of the report as day, month, year, or month, year. If more than one date appears on the report, use date of publication.

7a. TOTAL NUMBER OF PAGES: The total page count should follow normal pagination procedures, i.e., enter the number of pages containing information.

7b. NUMBER OF REFERENCES: Enter the total number of references cited in the report.

8a. CONTRACT OR GRANT NUMBER: If appropriate, enter the applicable number of the contract or grant under which the report was written.

8b, 8c, & 8d. PROJECT NUMBER: Enter the appropriate military department identification, such as project number, subproject number, system numbers, task number, etc.

9a. ORIGINATOR'S REPORT NUMBER(S): Enter the official report number by which the document will be identified and controlled by the originating activity. This number must be unique to this report.

9b. OTHER REPORT NUMBER(S): If the report has been assigned any other report numbers *(either by the originator or by the sponsor)*, also enter this number(s).

10. AVAILABILITY/LIMITATION NOTICES: Enter any limitations on further dissemination of the report, other than those imposed by security classification, using standard statements such as:

(1) "Qualified requesters may obtain copies of this report from DDC."

(2) "Foreign announcement and dissemination of this report by DDC is not authorized."

(3) "U. S. Government agencies may obtain copies of this report directly from DDC. Other qualified DDC users shall request through

_____."

(4) "U. S. military agencies may obtain copies of this report directly from DDC. Other qualified users shall request through

_____."

(5) "All distribution of this report is controlled. Qualified DDC users shall request through

_____."

If the report has been furnished to the Office of Technical Services, Department of Commerce, for sale to the public, indicate this fact and enter the price, if known.

11. SUPPLEMENTARY NOTES: Use for additional explanatory notes.

12. SPONSORING MILITARY ACTIVITY: Enter the name of the departmental project office or laboratory sponsoring *(paying for)* the research and development. Include address.

13. ABSTRACT: Enter an abstract giving a brief and factual summary of the document indicative of the report, even though it may also appear elsewhere in the body of the technical report. If additional space is required, a continuation sheet shall be attached.

It is highly desirable that the abstract of classified reports be unclassified. Each paragraph of the abstract shall end with an indication of the military security classification of the information in the paragraph, represented as *(TS), (S), (C), or (U)*.

There is no limitation on the length of the abstract. However, the suggested length is from 150 to 225 words.

14. KEY WORDS: Key words are technically meaningful terms or short phrases that characterize a report and may be used as index entries for cataloging the report. Key words must be selected so that no security classification is required. Identifiers, such as equipment model designation, trade name, military project code name, geographic location, may be used as key words but will be followed by an indication of technical context. The assignment of links, rules, and weights is optional

GPO 886-551

UNCLASSIFIED

Security Classification